PARAMETRIC IDENTIFICATION FOR SHIP ROLL MOTION

YANMING ZHANG

Parametric Identification for Ship Roll Motion

by

© Yanming Zhang, B. Eng., M. Eng.

A thesis submitted to the School of Graduate Studies
in partial fulfillment of the requirements
for the degree of Master of Engineering

Faculty of Engineering and Applied Science
Memorial University of Newfoundland

July 1993

St. John's Newfoundland Canada

ISBN 0-315-86624-1

Canada

Abstract

This Thesis presents a systematic study of the parametric identification and probability description of ship roll motion. A new method for parametric identification using modulating function technique is proposed. The method provides an easier way of solving a wide range of ship roll parametric identification problems including parametric identification from free roll decay data, forced roll data and randomly excited roll data. Another advantage is that it can be used to estimate the parameters of nonlinear damping moment, nonlinear-time-dependent restoring moment and the strength of excitation from measured roll response without necessarily knowing the excitation. This makes the prediction of ship dynamic stability possible because the ship roll parameters can be obtained from only the roll response of a ship. Furthermore, the new method avoids a main source of computational error which results from the numerical differentiation of the measured data which is used by many current parametric identification methods, and therefore it can produce more accurate results.

The second part of the work deals with the probability description of roll motion. From estimated roll parameters, the joint probability distribution of roll angle and velocity as well as probability distribution of peaks of roll motion are derived using the Markov approximation.

The method has been validated by applying it to analyse several ship roll data including the following, (1) experimental roll data of four ship models; (2)

numerically simulated roll data; (3) measured roll data of a full scale ship at sea. In all the above applications, the proposed method has been found to produce more satisfying results.

The probability distributions of the roll angle, roll velocity and peaks of roll motion obtained by a numerical approximation also show a good agreement with the relevant histograms of the experimental data. All these results suggest that the proposed method is a successful approach for the ship roll motion study.

Acknowledgements

I would like to thank my supervisor, Dr. M. R. Haddara for his support and guidance during this research.

I wish to extend my thanks and appreciation to Dr. J. J. Sharp and Dr. T. Chari for providing funding and teaching assistantships.

The assistance from Mr. D. Press and his staves at C-CAE is also appreciated.

My sincere thanks also go to Mr. B. Zou, Ms. X. Wu, Mr. S. Zhang, Mr. Z. Wang and Mr. N. Amoah for providing ship model test data and other relevant information.

Finally, I would like to thank my dear wife, Beiming, for her patience, love and understanding.

Contents

Abstract ii

Acknowledgements iv

List of Tables viii

List of Figures ix

1 Introduction 1

1.1 Ship Roll Motion 1

1.2 Parametric Identification of Ship Roll Motion 2

1.2.1 Parametric Identification from Free Roll Decay Data . . . 2

1.2.2 Parametric Identification from Forced Roll Data 3

1.2.3 Parametric Identification from Random Roll Data 5

1.3 Parametric Identification Method Using the Modulating Function Technique 7

1.4 Probability Description of Ship Roll Motion 8

2 System Identification Using the Modulating Function Technique 10

2.1 Problem Formulation 10

2.2 Modulating Function Technique 12
2.3 Choice of Modulating Functions 16

3 Estimation of Ship Roll Parameters from Forced Roll Response 20
3.1 Method of Solution 20
3.2 Improvements of Solution Accuracy 23
3.2.1 Numerical Integration 23
3.2.2 A More Efficient Difference Formula 25
3.2.3 Linear-Angle-Dependence Nonlinear Damping 26
3.3 Examples and Results 27
3.3.1 Numerically Simulated Data 27
3.3.2 Roll Motion in Regular Beam Waves 28
3.4 Discussion 30

4 Estimation of Ship Roll Parameters from Free Roll Decay Curves 33
4.1 Analysis of Free Roll Decay Data 33
4.2 Examples and Results 34
4.2.1 Simulated Data 34
4.2.2 Experimental Data 34
4.3 Discussion 40

5 Estimation of Ship Roll Parameters from Roll Response in Random Waves 46
5.1 Introduction 46
5.2 Parametric Identification 48
5.2.1 Autocorrelation Equation 48

5.2.2 Equation for the Random Decrement 49
5.2.3 Modulating Function Operation 51
5.3 Examples and Results 51
5.3.1 Simulated Data 51
5.3.2 Experimental Data 53
5.3.3 Full Scale Ship Roll Data 55

6 Probability distribution of Roll Motion **63**
6.1 Introduction 63
6.2 Markov Approximation and Solution 64
6.3 Peak Statistics 69
6.4 Results and Discussion 70
6.4.1 Duffing's Equation 70
6.4.2 Measured Data 72

7 Conclusions **79**

References **81**

Appendices **85**

A A and B Matrixes **86**

B Expression for $\frac{\partial}{\partial t}(G^{pq})$ **88**

C Data of Ship Models and Full Scale Ship **89**

List of Tables

3.1 Comparison of two integrations 25

3.2 Comparison between estimated parameters and their true values . 29

3.3 Estimated parameters from experimental data 29

4.1 Comparison between estimated and given parameters 34

4.2 Parameters estimated for Model 363 35

4.3 Parameters estimated for Model 365: First part 36

4.4 Parameters estimated for Model 365: Second part 37

4.5 Parameters estimated for Model 366: First part 38

4.6 Parameters estimated for Model 366: Second part 39

5.1 Estimated parameters and their true values 52

5.2 Estimated parameters of Model 366 (GM=4.91cm) 54

5.3 Estimated parameters of Model 365 (GM=4.31cm) 55

5.4 Estimated parameters of Model 363 (GM=3.10cm) 55

5.5 Estimated parameters about full scale ship 56

6.1 Parameters used in the calculation 71

C.1 Particulars of ship models 90

C.2 General particulars of a full scale ship 91

List of Figures

2.1 Roll angle record 18

2.2 $A^n(t)$ functions 18

2.3 Modulating function operation: A 19

2.4 Modulating function operation: B 19

3.1 Comparison of two numerical difference formulas 31

3.2 Simulated $\varphi(t)$ curve (Data set A) 31

3.3 Simulated $\varphi(t)$ curve (Data set B) 32

3.4 Comparison of experimental data and reproduced $\varphi(t)$curve of forced roll motion 32

4.1 Comparison of estimated and experimental roll curves for Model 363 41

4.2 Comparison of estimated and experimental roll curves for Model 365 41

4.3 Comparison of estimated and experimental roll curves for Model 366 42

4.4 A_0 vs. GM of Model 363 42

4.5 A_0 vs. GM of Model 365 43

4.6 A_0 vs. GM of Model 366 43

4.7 Roll damping vs. initial angle for different GM values (Model 363) 44

4.8 Roll damping vs. initial angle for different GM values (Model 365) 44

4.9 Roll damping vs. initial angle for different GM values (Model 366) 45

5.1 Variations of roll moment and roll response for simulated data . . 57

5.2 Spectrum of roll moment and roll response for simulated data . . 57

5.3 Comparison between different estimation 58

5.4 Comparison of magnitudes of crosscorrelation and autocorrelation 58

5.5 Comparison between calculated autocorrelation and experimental results for case A 59

5.6 Comparison between calculated random decrement and experimental results for case C 59

5.7 Comparison between calculated and experimental roll angle for case D 60

5.8 Relationship between GM and A_0 for full scale ship 60

5.9 Comparison between calculated and experimental autocorelation of real ship (GM=0.6989) 61

5.10 Comparison between calculated and experimental autocorelation of real ship (GM=0.7091) 61

5.11 Comparison between calculated and experimental autocorelation of real ship (GM=0.7287) 62

6.1 A-level crossing of $p(\varphi)$ 73

6.2 $\nu_a^+ dt = P(\frac{a-\varphi(t)}{dt} < \dot{\varphi}(t) < \infty)$ 73

6.3 Comparison between estimated and analytical probability distribution for Case A 74

6.4 Comparison between estimated and analytical probability distribution for Case *B* 74
6.5 Comparison between estimated and analytical probability distribution for Case *C* 75
6.6 Comparison between estimated roll angle distribution to the histogram of measured data for Model 366 75
6.7 Comparison between estimated roll velocity distribution to the histogram of measured data for Model 366 76
6.8 Comparison between estimated peak distribution to the histogram of measured data for Model 366 76
6.9 Comparison between estimated roll angle distribution to the histogram of measured data for full scale ship 77
6.10 Comparison between estimated roll velocity distribution to the histogram of measured data for full scale ship 77
6.11 Comparison between estimated peak distribution to the histogram of measured data for full scale ship 78

C.1 Body plan of Model 363 92
C.2 Body plan of Model 365 92
C.3 Body plan of Model 366 93
C.4 Body plan of Model 367 93
C.5 Full scale ship layout 94

Chapter 1

Introduction

1.1 Ship Roll Motion

The study of ship motions at sea is very important for ship stability and safety. Of all ship motions, the roll motion is the most crucial and the most difficult one to predict. The roll motion of a ship, in some situations, may reach dangerously large amplitudes and can result in capsizing of the ship. Modern hydrodynamic theories based on potential flow assumptions can give reasonable prediction of the ship motions with the exception of the roll motion, The roll damping is mainly caused by the viscosity of water which is not accounted for in the potential flow. One way for estimating the ship roll characteristics is to employ parametric identification methods. In these methods, the roll motion is assumed to be governed by a second-order differential equation whose parameters are to be determined. These parameters can be estimated from free roll decay test or, in a more resonable way, from measured roll data of a ship traveling at sea.

The main purpose of the present study is to find a method which can estimate roll parameters of a ship at sea. The estimation by the method should only

depend on the measured roll angle records, because other information, such as the excitation from waves, is difficult to be obtained. From the estimated roll parameters, the ship stability can be assessed.

1.2 Parametric Identification of Ship Roll Motion

The pioneering work of Froude [1] marked the start of ship roll parametric estimation. Many studies followed which ranged from simple to complicated approaches and from a linear approximation to nonlinear approach. Most early studies were focused on the estimation of roll parameters from free roll decay tests, which is relatively simple. The deficiency in the early work is that the parameters estimated from free roll tests in calm water may change when the ship loading or other conditions change. Only in recent years, more attention is being paid to the estimation of roll parameters from forced roll data.

1.2.1 Parametric Identification from Free Roll Decay Data

Different methods can be used for the analysis of free roll decay test data to estimate roll parameters. Froude [1] proposed an energy method to obtain damping parameters by equating the energy loss of the damping to the work done by the restoring moment. Since the estimation relies on the slope of the decay curve, this makes the method sensitive to the precise amplitude at the start of the curve.

Roberts developed the Froude method to a new energy method [2], which can handle the nonlinear restoring moment terms in the roll equation. Improvements

are still needed for applying this method to the measured roll data with noise, because it is "critically dependent on the success of the fairing process" of the experimental data [3].

The DEFIT method and the energy approach proposed by Bass and Haddara [4] show an advantage, that the information of whole roll curve, not only the peak values, can be used for the estimation. Thus the roll parameters can be estimated from a relatively short record.

In reference [5] (Bass and Haddara), a particular study was presented for ship roll damping identification of some small fishing vessels. The investigations include not only the roll damping but also the roll-sway coupled damping.

One of the main sources of error in the estimation, in many current methods, is the process of the numerical differentiation of experimental data. The method proposed in this thesis uses numerical integration instead of numerical differentiation to handle the roll equation, so the accuracy of the estimation can be improved.

The analysis of the experimental roll data for three ship models by the proposed method is presented in Chapter 4. Using the estimated parameters, the linear relationship between the natural frequencies of roll motion and the values of metacentric height as well as the relationship between maximum amplitudes of roll angle and the damping parameters are demonstrated.

1.2.2 Parametric Identification from Forced Roll Data

Forced roll motion usually refers to the roll motion with a single sinusoidal wave excitation, such as the roll motion of a ship in regular beam waves. As mentioned before, it is not certain whether the parameters obtained from free roll

decay test in calm water can be used to provide accurate predictions of the roll motion of a ship at sea. At least it is true, that the restoring moment of a ship at sea will change when the ship loading changes. It is desirable to develop a method which can estimate the ship roll parameters from the dynamic response of a ship under certain excitation.

Sponge [3] compared three methods which are available for the analysis of forced roll experiments, from which the model's nonlinear roll damping parameters can be determined. The three methods are a quasi-linear method, an energy method and a perturbation method. The third method was found impractical. The other two methods, which are only slightly different, produced better results. However, because both methods are based on the equivalent linear approximation, even for numerically simulated data, the estimation for nonlinear damping parameters by these methods is not accurate enough.

A method using system identification techniques was proposed by Gawthrop et al [6]. The method can be used to estimate roll parameters from forced roll motion, where the excitation moment is composed of some concatenated sine-waves. It is inconvenient to apply this method to the case of roll motion with a single sine-wave excitation such as the excitation from regular beam waves. The reason is that the method is based on the *linear* estimation scheme. A single sine-wave excitation can not provide enough information for the estimation of all roll parameters by this scheme.

The energy method developed by Haddara [7] can also be used for the analysis of forced roll data. An example was given for the identification of roll parameters from numerically simulated roll data with a single sine-wave excitation.

The method propose . by Zhang and Haddara [8] shows some advantages over other available methods. Such as, it can be used to estimate the parameters of the nonlinear restoring and damping moments as well as the strength and phase of the excitation moment from measured roll response only. Moreover, the estimation scheme allows the excitation to be a single sine-wave, a sum of sine-waves or in other forms. Other important improvement is on the accuracy of the estimation due to the high efficiency of the modulating function technique.

In Chapter 3, this method has been tested by applying it to the analysis of numerically simulated roll data and roll data measured from ship model tests in regular beam waves. In both cases, the method give very good estimation of all roll parameters. From the numerically simulated data, the nonlinear damping and nonlinear-time-dependent restoring moment characteristics as well as the amplitudes and phases of two sine-wave excitations are estimated at the same time with a high accuracy.

1.2.3 Parametric Identification from Random Roll Data

It is a complicated problem to estimate the roll parameters from random roll data. The difficulty is due to both the nonlinearities in the roll equation and the random excitation. Kountzeris et al [9] employed the same system identification method used in reference [6] to solve the problem. Because the method needs wave elevations in the vicinity of the ship as an input data for the parametric identification, it is difficult to apply it in practice.

Roberts [10] proposed a method based on the Markov property of the energy envelope process to solve the same problem. In the method, white noise excitation and light damping assumptions are used. Moreover, the energy envelope used

in the method is calculated from the roll velocity, the accurate value of which is very difficult to be obtained from measured roll data with noise. For some numerically simulated roll data, the method produced reasonable but not very good estimation. No examples are found to apply this method to the analysis of experimental data.

The random decrement technique has been used sucessfully in the damping identification of linear systems. Haddara [11] developed this technique using the concept of Markov approximation and made it applicable to nonlinear systems arising in the ship roll problems. The basic assumption underlying the Markov approximation is that the dynamic system has no memory. The equation for random decrement has the same form as the free decay roll equation. This contribution is very useful because the parametric identification from random roll motion can be handled in the same way as the parametric identification from free decay roll motion.

Reference [12] (Wu) presents some work of the parametric estimation from random roll data using the random decrement technique. The white noise excitation assumption is also used. The equation for the random decrement used in the study can be considered as the first order approximation of the random decrement equation used in the present work.

All of the above methods work only in limited range of roll problems. No method exists in the literature which can be used for the estimation of the roll parameters from the roll motion of a ship in random oblique waves.

In this thesis, an equation derived from the original roll equation is used for the parametric identification. This equation may be an equation for autocorrelation

of roll angle or an equation for random decrement of roll angle. The advantage of this transformation is that the study of a random differential equation can be shifted to the study of an ordinary differential equation without introducing any approximation.

This method does not need the Markov approximation and the assumption of white noise excitation, so a more realistic narrow-band excitation is used in the study. [13]

In Chapter 5, the method has been used for the analysis of a series of ship roll data: the roll data of three ship models subjected to random wave excitation, the numerically simulated roll data with a narrow-band random excitation, and the measured roll data of a full scale fishing vessel at sea. Both autocorrelation equation and random decrement equation are used for the parametric estimation. The calculated results indicate that the present method is a simple yet an efficient estimation procedure.

1.3 Parametric Identification Method Using the Modulating Function Technique

The ship roll equation is of the same form as an equation of a single input-output system popularly seen in automatic control engineering field. Our parametric identification method is also developed from a system identification method using modulating function technique [14], which has been known for some time in the field of automatic control engineering. This method is designed for the parametric identification from a linear system using both input and output signals. Similar to Fourier transform, it can transform a differential equation to

an algebraic equation, so the differentiation of the measured data in the system equation can be avoided. It also shows other merits such as linear, no iteration and no cutoff error. In the ship roll problem, the input signal representing the wave excitation moment is unknown, so some extensions are needed to apply this method. The solution is to model the real excitation moment by a numerically generated excitation moment with the condition that the assumed excitation moment should have a similar spectrum density distribution and strength as that of the original excitation moment. The strength of this assumed excitation moment is to be determined from the roll response data.

It is the first time, to the author's knowledge, to introduce the system identification method using modulating function technique into the ship roll problem. The present method is the only known method which can estimate nonlinear damping, nonlinear-time-dependent restoring parameters and the strength of excitation moment from the roll response only.

More details about the derivation of the method and the modulating function technique can be found in Chapter 2.

1.4 Probability Description of Ship Roll Motion

If the extreme values of roll angle can be predicted, many ship losses may be avoided by taking appropriate precaution. To predict the probability distribution of roll angle, roll velocity and peaks of roll motion from the estimated roll parameters is another part of the present study. For such a nonlinear random vibration problem, the exact solution is only available for a limited number of

simple cases. Therefore, considerable efforts have gone into the development of approximations and numerical methods. The most powerful method for determining the probability structure of the response of a nonlinear system is based on the Markov approximation with the assumption that the input is a white noise. In this case, the transition probability of the response satisfies the Fokker-Planck equation [15]. The exact solution of this equation can be found only for a few cases [16]. To avoid solving this equation directly, Haddara [17] has derived a set of approximate equations for the mean and variance of roll angle and velocity.

In this thesis, the Galerkin Method is used to solve the Fokker-Planck equation [18]. Using estimated roll parameters, the solutions give the probability distribution of roll angle, roll velocity and peaks of roll angle. The calculated results are then compared with the analytical solutions of a special case and good agreement is observed. The calculated results are also compared with the histograms of roll motion extracted from the experimental data of ship models and the measured data of a full scale ship, and good agreement is also obtained.

More details about this work are presented in Chapter 6.

Chapter 2

System Identification Using the Modulating Function Technique

2.1 Problem Formulation

The roll motion of a ship subjected to an excitation moment $M(t)$ can be described by the following second-order ordinary differential equation:

$$I\ddot{\varphi} + C(\dot{\varphi}) + D(\varphi, t) = M(t) \tag{2.1}$$

where I is the virtual mass roll moment of inertia of the ship and φ is the roll angle. $C(\dot{\varphi})$, $D(\varphi, t)$ are nonlinear damping and restoring moments, respectively. A dot over the variable means the differentiation with respect to time.

The damping moment has been classically represented as follows,

$$C(\dot{\varphi}) = \alpha\dot{\varphi} + \beta\dot{\varphi}|\dot{\varphi}| \tag{2.2}$$

The restoring moment $D(\varphi, t)$ is usually expressed as an odd polynomial in the angle of roll $\varphi(t)$. To include the effect of time variations in the restoring moment caused by oblique or following waves, we write the restoring moment as:

$$D(\varphi,t) = (1 + \delta sin(\omega t))(\mu_1\varphi + \mu_2\varphi^3 + \mu_3\varphi^5) \qquad (2.3)$$

where μ_1, μ_2, μ_3 are linear and nonlinear coefficients of restoration terms; δ and ω are, respectively, the amplitude and frequency of the time-dependent variation in the restoration. In this expression, the roll motion is considered to be decoupled with other motions of the ship.

Dividing equation (2.1) by I , the governing equation of roll motion becomes:

$$\ddot{\varphi} + B_0\dot{\varphi} + B_1\dot{\varphi}|\dot{\varphi}| + (1 + \delta sin(\omega t))(A_0\varphi + A_1\varphi^3 + A_2\varphi^5) = KM(t) \qquad (2.4)$$

where

$$B_0 = \frac{\alpha}{I} \quad B_1 = \frac{\beta}{I} \quad A_0 = \frac{\mu_1}{I} \quad A_1 = \frac{\mu_2}{I} \quad A_2 = \frac{\mu_3}{I} \quad K = \frac{1}{I} \qquad (2.5)$$

The main objective of this work is to find a method for the prediction of the variables in equation (2.4) from the measured record of roll angle $\varphi(t)$. One of the methods that can be used for this purpose is the Energy Method [19]. However, a major disadvantage of this method is that it depends on the calculation of the roll velocity from the roll angle record using numerical differentiation. This is a drawback when dealing with noisy records similar to the one shown in Figure 2.1. Methods which depend on numerical integration instead of numerical differentiation in the formulation of the prediction equations usually provide superior results. Another factor that should be observed is that the prediction equations should provide sufficient information for the estimation of all unknown parameters

at hand (see Gawthrop [6]). The modulating function technique discussed in the next section has these advantages.

2.2 Modulating Function Technique

The modulating function technique is used to solve the equation of linear systems in the realm of automatic control engineering using input and output data [14]. In this work, it is applied to a nonlinear system. A further extension is to use this technique to predict parameters from the measured output data only. Wave elevations representing the input data, in the case of ship motion at sea, are difficult to obtain.

Similar to Fourier and Laplace transforms, the principle of the modulating function technique is to convert the system differential equation into a simple algebraic equation. The modulating function operator is defined as:

$$\Psi_n(\varphi(t)) = \int_{-\infty}^{\infty} \varphi(t) A^n(t) dt \tag{2.6}$$

where $A^n(t)$ is the modulating function and $\varphi(t)$ is the output signal of the system.

If $A^n(t)$ is chosen to be e^{-int}, the modulating function operation is simply the Fourier transform. In this work, $A^n(t)$ is chosen to be the weighted Hermite function defined as:

$$A^n(t) = e^{-\frac{t^2}{2}} H_n(t) = (-1)^n \frac{d^n}{dt^n}(e^{-\frac{t^2}{2}}) \tag{2.7}$$

where $H_n(t)$ is a Hermite polynomial of order n, given as:

$$H_n(t) = (-1)^n e^{\frac{t^2}{2}} \frac{d^n}{dt^n}(e^{-\frac{t^2}{2}}) \tag{2.8}$$

Using equation (2.7), one can show that the rth-order derivative of A^n can be expressed as:

$$\frac{d^r A^n}{dt^r} = (-1)^r A^{n+r} \tag{2.9}$$

The modulating function operation on the derivative of $\varphi(t)$ is given as:

$$\Psi_n(\frac{d\varphi}{dt}) = \int_{-\infty}^{\infty} \frac{d\varphi}{dt} A^n dt \tag{2.10}$$

Because $A^n(\pm\infty) = 0$, integrating equation (2.10) by parts gives,

$$\Psi_n(\frac{d\varphi}{dt}) = \int_{-\infty}^{\infty} \varphi A^{n+1} dt = \Psi_{n+1}(\varphi) \tag{2.11}$$

Similarly, for higher order derivatives, one has,

$$\Psi_n(\frac{d^r\varphi}{dt^r}) = \Psi_{n+r}(\varphi) \tag{2.12}$$

In this way, a differential operator is converted to an algebraic operator.

Consider a linear system given by

$$\sum_{m=0}^{L} a_m \frac{d^m\varphi}{dt^m} = \sum_{i=1}^{K} d_i M_i(t) \tag{2.13}$$

where $M_i(t)$ is the input to the system.

Applying modulation function operation to each side of this equation, one gets the following algebraic equation:

$$\sum_{m=0}^{L} a_m \Psi_{m+n}(\varphi) = \sum_{i=1}^{K} d_i \Psi_n(M_i(t)) \tag{2.14}$$

Without loss of generality, a_L can be set to unity. Letting n change from 1 to $L+K$, the unknowns $[a_0, a_1, ...a_{L-1}, d_1, d_2, ...d_K]$ can be obtained from the $L+K$ independent simultaneous algebraic equations:

$$\sum_{m=0}^{L-1} a_m \Psi_{m+n}(\varphi) - \sum_{i=1}^{K} d_i \Psi_n(M_i(t)) = -\Psi_{L+n}(\varphi) \tag{2.15}$$
$$(n = 1, 2, ..., \ L+K)$$

Inspection of equation (2.15) shows that no differentiation of the output function $\varphi(t)$ is needed. The known coefficients in the above equations are modulating function integrations on the recorded data.

In practice, it is impossible to get an infinite record. The finite integration limits can be used because $A^n(t)$ approaches zero very fast as $|t|$ increases (see Figure 2.2). A limit T_∞ can be given such as:

$$e^{-\frac{T_\infty^2}{2}} T_\infty^m < 10^{-8} \tag{2.16}$$

where $m = max[n]$, and n is the highest order of $A^n(t)$.

This means when $T = T_\infty$, $A^n(t)$ will be less than 10^{-8}.

In this work, a coordinate transformation is adopted. The modulating function operation is defined as:

$$\Psi_n(\varphi(t)) = \int_0^T \varphi(t) A^n(\tau) dt \tag{2.17}$$

$$\begin{aligned}\Psi_n(\frac{d\varphi}{dt}) &= \int_0^T \frac{d\varphi}{dt} A^n(\tau) dt \\ &= T_r \Psi_{n+1}(\varphi(t)) + \varphi(T) A^n(T_e) - \varphi(0) A^n(-T_s)\end{aligned} \tag{2.18}$$

$$\begin{aligned}\Psi_n(\frac{d^2\varphi}{dt^2}) &= \int_0^T \frac{d^2\varphi}{dt^2} A^n(\tau) dt \\ &= T_r{}^2 \Psi_{n+2}(\varphi(t)) + \frac{d\varphi}{dt}|_T A^n(T_e) - \frac{d\varphi}{dt}|_0 A^n(-T_s) \\ &\quad + T_r \varphi(T) A^{n+1}(T_e) - \varphi(0) A^{n+1}(-T_s)]\end{aligned} \tag{2.19}$$

where

$$\tau = T_r t - T_s, \qquad T_r = \frac{T_e + T_s}{T}$$

and T is the length of the record $\varphi(t)$.

T_e, T_s can be chosen by the user in order to move the weight on φ in the integration. For example, in the case of free roll, the first several cycles are considered to be more accurate, so T_s can be set to zero and $T_e = T_\infty$. This means that the largest weight is put on the part at the beginning of the record. (see Figure 2.3). If the boundary values of φ and $\dot{\varphi}$ are unknown or unimportant, T_e and T_s can be assumed equal to T_∞ (see Figure 2.4). In this case:

$$\Psi_n(\frac{d\varphi}{dt}) = T_r \Psi_{n+1}(\varphi) \tag{2.20}$$

$$\Psi_n(\frac{d^2\varphi}{dt^2}) = (T_r)^2\Psi_{n+2}(\varphi) \tag{2.21}$$

The modulating function technique has the following advantages:

1. Generalization : The method can be used to estimate parameters from a general form of ship roll equation provided that the unknown parameters are not associated with time t. For example, if one of the terms in the equation is $A_0 sin(\omega t + \delta)$, A_0 and δ can be easily predicted using this method but prediction of ω is difficult.

2. Accuracy and Stability: because the method is based on the integration of measured data , the results are less sensitive to the noise in the measurements or to the errors introduced by a numerical differentiation.

2.3 Choice of Modulating Functions

First, the algebraic equations for the solution of parameters must be independent. This condition is satisfied if the modulating functions were orthogonal to each other.

The modulating functions A^n chosen in this work satisfy the following orthogonality condition:

$$\int_{-\infty}^{\infty} e^{\frac{t^2}{2}} A^n(t)A^m(t)dt = \delta_{nm}\sqrt{2\pi}n! \qquad \delta_{nm} = \begin{cases} 1 & (n = m) \\ 0 & (n \neq m) \end{cases} \tag{2.22}$$

Second, if the exact values of the output data $\varphi(t)$ at the ends $[0, T]$ of the record can not be easily obtained, it is desirable to have the following condition:

$$A^n(0) = A^n(T) = 0 \tag{2.23}$$

The present modulating function also satisfies this condition.

Other properties are also needed. For example, a function of the form

$$A^n(t) = sin(n\pi\frac{t}{T}) \tag{2.24}$$

satisfies the orthogonality condition, but it is not a good choice as a modulating function. The reason is that when n is very large this function is a highly oscillating function, and the integration

$$\int_0^T \varphi(t)\sin(n\pi\frac{t}{T})dt \tag{2.25}$$

approaches zero.

The modulating function technique has been known in the field of automatic control engineering for some time. It is essentially used to predict the parameters of linear systems through relating the input to the output of the systems. The new approach in this work is to use this method to predict parameters in the nonlinear roll equation using only output information. No information about the input is needed. More details about this approach will be discussed in the following Chapters.

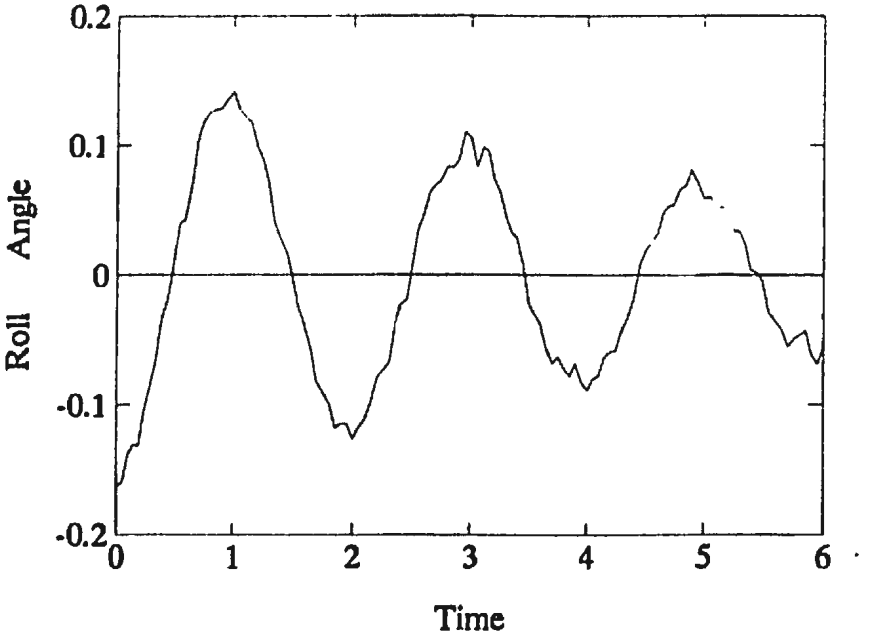

Figure 2.1: Roll angle record

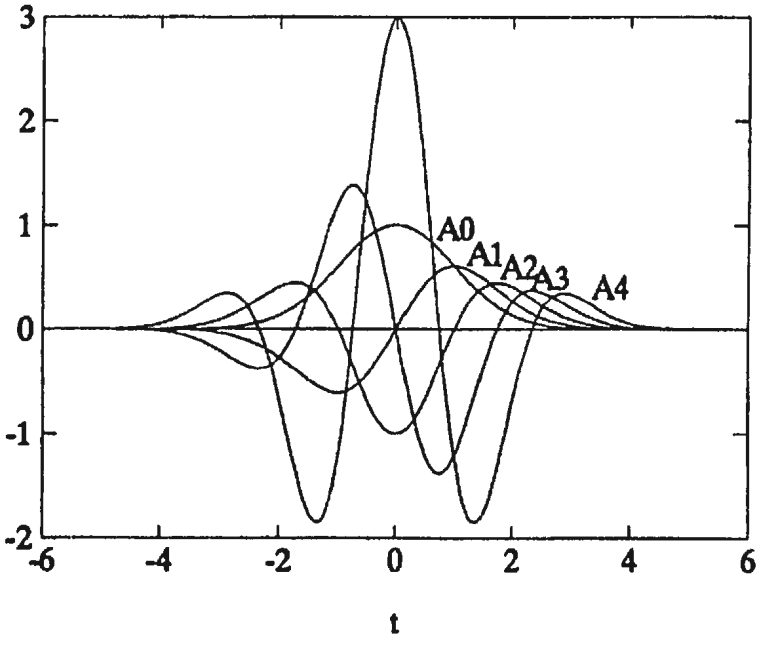

Figure 2.2: $A^n(t)$ function

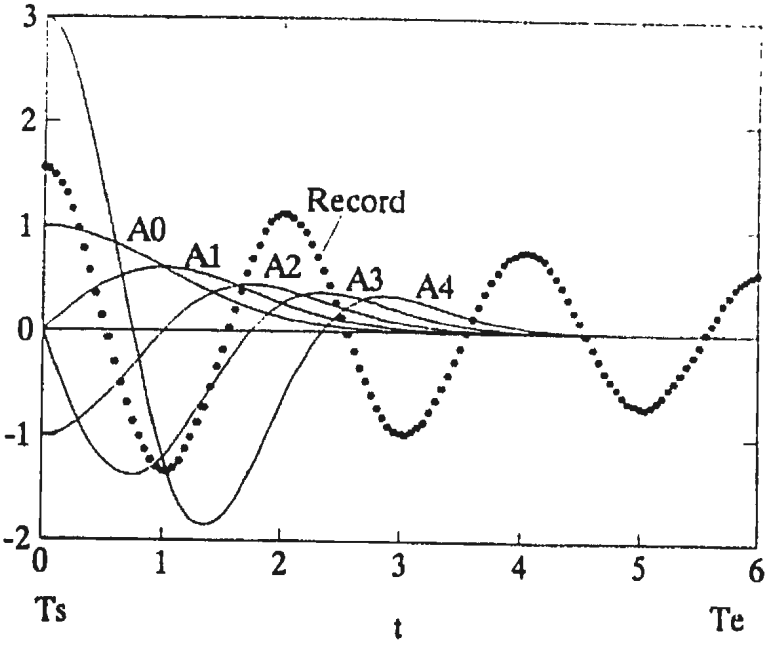

Figure 2.3: Modulating function operation: A

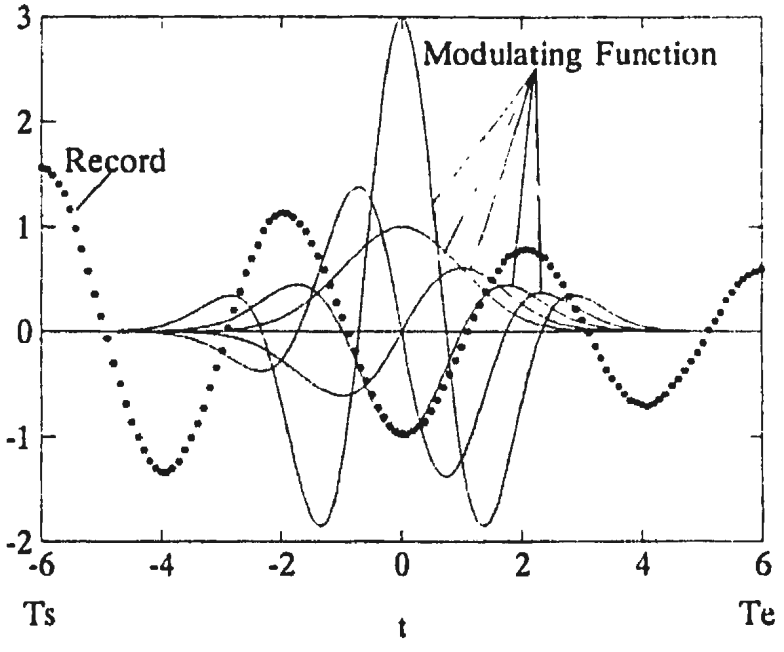

Figure 2.4: Modulating function operation: B

Chapter 3

Estimation of Ship Roll Parameters from Forced Roll Response

3.1 Method of Solution

The equation of ship roll motion in regular oblique waves can be obtained from equation (2.4) by substituting the following expression for the exciting moment:

$$KM(t) = D_1 sin(\Omega_1 t + \gamma_1) \tag{3.1}$$

where D_1 is the moment amplitude, Ω_1 is the wave frequency of encounter and γ_1 is the phase of the excitation moment.

If the excitation is caused by irregular waves, the excitation moment can be expressed approximately as:

$$KM(t) = \sum_{i=1}^{m} D_i sin(\Omega_i t + \gamma_i) \tag{3.2}$$

Substituting this expression into equation (2.4), we have

$$\ddot{\varphi} + B_0\dot{\varphi} + B_1\dot{\varphi}|\dot{\varphi}| + (1 + \delta sin(\omega t))(A_0\varphi + A_1\varphi^3 + A_2\varphi^5)$$
$$= \sum_{i=1}^{m} D_i sin(\Omega_i t + \delta_i) \tag{3.3}$$

The above equation can also be written as:

$$\begin{aligned}&\ddot{\varphi} + B_0\dot{\varphi} + B_1\dot{\varphi}|\dot{\varphi}| + A_0\varphi + \overline{A_0}sin(\omega t)\varphi \\ &+A_1\varphi^3 + \overline{A_1}sin(\omega t)\varphi^3 + A_2\varphi^5 + \overline{A_2}sin(\omega t)\varphi^5 \\ &= \sum_{i=1}^{m}[C_i sin(\Omega_i t) + S_i cos(\Omega_i t)] \end{aligned} \tag{3.4}$$

where

$$\overline{A_0} = A_0\delta \tag{3.5}$$

$$\overline{A_1} = A_1\delta \tag{3.6}$$

$$\overline{A_2} = A_2\delta \tag{3.7}$$

$$C_i = D_i cos(\gamma_i) \tag{3.8}$$

$$S_i = D_i sin(\gamma_i) \tag{3.9}$$

If all the parameters $B_0, B_1, A_0, A_1, A_2, \overline{A_0}, \overline{A_1}, \overline{A_2}, C_i, S_i$ are known, a solution of equation (3.4) yields $\varphi(t)$ for each Ω_i and ω.

Applying the modulating function operation on equation (3.4) and letting the order of modulating function operation n to vary from 0 to L, (*where* $L = 2m+7$), a set of algebraic equations are obtained as:

$$\begin{aligned}&\overline{\Psi_{n+2}(\varphi)} + B_0\overline{\Psi_{n+1}(\varphi)} + B_1\Psi_n(\dot{\varphi}|\dot{\varphi}|) + A_0\Psi_n(\varphi) + A_1\Psi_n(\varphi^3) + A_2\Psi_n(\varphi^5) \\ &+\overline{A_0}\Psi_n(sin(\omega t)\varphi) + \overline{A_1}\Psi_n(sin(\omega t)\varphi^3) + \overline{A_2}\Psi_n(sin(\omega t)\varphi^5) \\ &= \sum_{i=0}^{m}[C_i\Psi_n(sin(\Omega_i t)) + S_i\Psi_n(cos(\Omega_i t))] \qquad (n = 0, 1, 2... , L) \end{aligned} \tag{3.10}$$

where

$$\Psi_n(\varphi) = \int_0^T \varphi(t) A^n(T_r t - T_s) dt \tag{3.11}$$

$$\begin{aligned} \overline{\Psi_{n+1}(\varphi)} &= \int_0^T \frac{d\varphi}{dt} A^n(T_r t - T_s) dt \\ &= T_r \Psi_{n+1}(\varphi) + \varphi(T) A^n(T_e) - \varphi(0) A^n(-T_s) \end{aligned} \tag{3.12}$$

$$\begin{aligned} \overline{\Psi_{n+2}(\varphi)} &= \int_0^T \frac{d^2\varphi}{dt^2} A^n(T_r t - T_s) dt \\ &= {T_r}^2 \Psi_{n+2}(\varphi) + \frac{d\varphi}{dt}|_T A^n(T_e) - \frac{d\varphi}{dt}|_0 A^n(-T_s) \\ &\quad + T_r[\varphi(T) A^{n+1}(T_e) - \varphi(0) A^{n+1}(-T_s)] \end{aligned} \tag{3.13}$$

and

$$T_r = \frac{T_e + T_s}{T}$$

Equation (3.10) can also be written in a matrix form:

$$\mathbf{A}\theta = \mathbf{B} \tag{3.14}$$

θ is the vector of unknown parameters given as:

$$\theta = [B_0, B_1, A_0, A_1, A_2, \overline{A_0}, \overline{A_1}, \overline{A_2}, C_1, \ldots, C_m, S_1, \ldots, S_m]^T$$

The expressions of **A**, **B** can be found in Appendix A.

If more quations are used, that is, letting the order of modulating function to vary from 0 to M, M is greater than $(2m + 7)$, then the matrix **A** is of ($(M + 1)$x$(L + 1)$) order. In this case, a least squares technique can be used.

All elements in matrix **A** except the second column are modulating function integrations on the measured records. They can be calculated using any numerical integration method, such as an ordinary Simpson numerical integration method.

The second column is modulating function integration on the nonlinear damping term, which includes the derivatives of the measured record. As mentioned before, it is not easy to accurately calculate the derivatives from measured records containing errors. We have successfully avoided to deal with the terms $\dot{\varphi}$, $\ddot{\varphi}$ in the roll equation. This is the only term left which includes derivatives.

Three approaches for calculating this term are discussed in the following section.

3.2 Improvements of Solution Accuracy

3.2.1 Numerical Integration

Define a function $F(t)$ as:

$$F(t) = \int_0^t \dot{\varphi}(u)|\dot{\varphi}(u)|du + Constant \tag{3.15}$$

then the modulating function operation on nonlinear damping term becomes,

$$\begin{aligned} \Psi_n(\dot{\varphi}|\dot{\varphi}|) &= \int_0^T \dot{\varphi}(t)|\dot{\varphi}(t)|A^n(\tau)dt = \int_0^T \frac{dF}{dt}A^n(\tau)dt \\ &= F(T)A^n(T_c) - F(0)A^n(-T_s) + T_r\int_0^T F(t)A^{n+1}(\tau)dt \end{aligned} \tag{3.16}$$

where

$$\tau = (T_c + T_s)\frac{t}{T} - T_s$$

$F(t)$ can be calculated from the measured data in the following way.

Near the ith point of the measured data, the roll angle can be approximated as:

$$\varphi_i(t) = a_i t^2 + b_i t + c_i \tag{3.17}$$

Then we have

$$\dot{\varphi}_i|\dot{\varphi}_i| = sign(\dot{\varphi}_i)(4a_i^2 t^2 + 4a_i b_i t + b_i^2) \tag{3.18}$$

$$F_i(t) = sign(\dot{\varphi}_i)(\frac{4}{3}a_i^2 t^3 + 2a_i b_i t^2 + b_i^2 t) + F_{i-1} \qquad (F_0 = 0) \tag{3.19}$$

where the coefficients a_i, b_i can be determined from the values of $\varphi_{i-1}, \varphi_i, \varphi_{i+1}$. The *sign* function means that the expression should has the same sign as the variable.

Because the nth modulating function operation on a constant is equal to zero when $n > 0$ and $T_s = T_e$, we set F_0 to zero.

To verify the improvement of the present modification, two expressions for $\Psi_n(\dot{\varphi}|\dot{\varphi}|)$, given in (3.20) and (3.21), are evaluated using order $n = 1$, namely

$$I_1 = \int_0^T \dot{\varphi}(t)|\dot{\varphi}(t)|A^1(\tau)dt \tag{3.20}$$

$$I_2 = F(T)A^1(T_e) - F(0)A^1(-T_s) + T_r \int_0^T F(t)A^2(\tau)dt \tag{3.21}$$

The following two expressions for $\varphi(t)$ are used in the evaluation of the two integrations.

Table 3.1: Comparison of two integrations

	A	B
Accurate Values	4.2803364	4.6153510
I_1	4.2451878	4.6075177
I_2	4.2800570	4.6153095

$$\textit{First expression } (A): \quad \varphi(t) = e^{-0.1t} sin(8t) \tag{3.22}$$

$$\textit{Second expression } (B): \quad \varphi(t) = sin(8t) \tag{3.23}$$

and

$$T = \frac{2.5\pi}{8} \qquad T_s = T_e = 6$$

From the discrete data, the derivatives in equation (3.20) are calculated using a two-point central difference formula.

Theoreticaly, the two integrations should give the same result. However, because of the difference in the numerical error, I_2 gives more accurate results as shown in Table 3.1. The "Accurate Values" in this Table are obtained by numerical integration on the exact $\dot{\varphi}(t)$ using very densely spaced discrete data.

The reason of this improvement is that $F(t)$ is the integration of nonlinear damping while the numerical integration generally has higher accuracy than numerical differentiation of the same discrete data. If there is noise in the $\varphi(t)$ data, this improvement will be more evident.

3.2.2 A More Efficient Difference Formula

In order to eliminate the random noise, a smooth-difference formula is devel-

oped.

Letting $\varphi_i(t) = a_i t^2 + b_i t + c_i$ at the vicinity of a point φ_i. The coefficients a_i, b_i, c_i can be determined from the values of $(\varphi_{i-2}, \varphi_{i-1}, \varphi_i, \varphi_{i+1}, \varphi_{i+2})$ using a least squares approach. The derivative of this function is

$$\dot{\varphi}_i(t) = 2a_i t + b_i \tag{3.24}$$

or

$$\dot{\varphi}_i = \frac{(68\varphi_{i+2} + 21\varphi_{i+1} - 6\varphi_i - 13\varphi_{i-1} - 70\varphi_{i-2})}{310\Delta t} \tag{3.25}$$

Figure 3.1 shows the comparison between the derivative (dashed line) calculated using above formula and the derivative (solid line) calculated using two-point central difference. It is obvious that the above formula gives more smooth and accurate representation of digital data.

3.2.3 Linear-Angle-Dependence Nonlinear Damping

As mentioned in reference [19], there are several expressions for the nonlinear roll damping. If a linear-angle-dependent nonlinear damping is adopted, the roll damping is,

$$C(\dot{\varphi}) = B_0\dot{\varphi} + B_1\varphi|\dot{\varphi}| \tag{3.26}$$

Applying modulating function operation on the nonlinear damping term results,

$$\Psi_n(|\varphi|\dot{\varphi}) = \int_0^T |\varphi|\dot{\varphi}A^n(\tau)dt$$

$$
\begin{aligned}
&= sign(\varphi)\int_0^T A^n(\tau)d(\frac{\tau^2}{2}) \\
&= sign(\varphi)(A^n(T_r)\frac{\tau^2}{2}|_T - A^n(-T_r)\frac{\tau^2}{2}|_0) \\
&\quad + sign(\varphi)T_r\Psi_{n+1}(\frac{\varphi^2}{2})
\end{aligned} \tag{3.27}
$$

In this way, no derivatives of the roll angle are needed.

In our calculation, the first two approaches give similar results which are better than the results calculated by the direct numerical differentiation method. The third approach has not been tested yet.

3.3 Examples and Results

3.3.1 Numerically Simulated Data

The first test case is on numerically simulated data. A roll motion equation (3.28) is integrated by a standard 4th-order $Runge-Kutta$ algorithm with two sets of given coefficients (sets A and B in table 3.2).

$$
\begin{aligned}
&\ddot{\varphi} + B_0\dot{\varphi} + B_1\dot{\varphi}|\dot{\varphi}| + (1 + \delta_1 sin(\omega_1 t) + \delta_2 sin(\omega_2 t))(A_0\varphi + A_1\varphi^3 + A_2\varphi^5) \\
&= D_1 sin(\Omega_1 t + \gamma_1) + D_2 sin(\Omega_2 t + \gamma_2)
\end{aligned} \tag{3.28}
$$

Two sets of simulated data $\varphi(t_i)$ are plotted in Figures 3.2 and 3.3. Since the time-dependent restoring moment is caused by waves, it should have the same frequencies as those of the waves. This is the condition in data set A. However, in data set B, we use different values for the frequency of waves and the frequency of the restoring moment.

For the integration interval $T = 10\ sec.$ with a uniform time step $\Delta t = 0.012$, 834 points of φ_i are obtained. From these data, the parameters are estimated using the mentioned method. Table 3.2 shows the comparison between the true values and the estimated values of these parameters. The agreement is seen to be very good.

3.3.2 Roll Motion in Regular Beam Waves

Experimental data were obtained from ship model tests in the wave tank at Memorial University of Newfoundland. The model used in the tests is a small fishing vessel Model 367. Its particalars can be found in Appendix C. The model was subjected to regular waves generated by a piston type generator. The waves have a wave height of 6 cm and a frequency of 0.45 Hz.

A total of 601 data points are recorded in 10 seconds. Table 3.3 shows the estimated parameters from the roll equation:

$$\ddot{\varphi} + B_0\dot{\varphi} + B_1\dot{\varphi}|\dot{\varphi}| + A_0\varphi + A_1\varphi^3 = D_1 sin(\Omega_1 t + \gamma_1) \tag{3.29}$$

Using these parameters, the $\varphi(t)$ curve is reproduced by numerical integration of equation (3.29). Figure 3.4 shows a very good agreement between the reproduced curve (solid line) and experimental curve (star marks).

Table 3.2: Comparison between estimated parameters and their true values

A : $\Omega_1 = 4.0 \quad \Omega_2 = 2.5 \quad \omega_1 = 4.0 \quad \omega_2 = 2.5$

B : $\Omega_1 = 2.0 \quad \Omega_2 = 2.5 \quad \omega_1 = 2.2 \quad \omega_2 = 2.6$

	Para.	B_0	B_1	A_0	A_1	A_2	δ_1	δ_2	D_1	D_2	γ_1	γ_2
A	*Given*	0.0400	0.7000	9.0000	1.0000	1.0000	0.6000	2.0000	1.0000	3.0000	0.4000	0.2000
A	*Esti.*	0.0395	0.7002	8.9968	1.0001	0.9915	0.5998	1.9999	1.0001	2.9999	0.4000	0.2002
B	*Given*	0.0500	0.5000	8.0000	1.0000	2.0000	0.1000	0.5000	2.0000	1.0000	0.2000	0.3000
B	*Esti.*	0.0500	0.5000	8.0001	1.0031	1.9956	0.1000	0.5001	2.0001	1.0000	0.1999	0.2998

Table 3.3: Estimated parameters from experimental data

B_0	B_1	A_0	A_1	D_1	γ_1
0.13718	0.58831	9.86965	-28.53927	0.27710	2.46352

3.4 Discussion

The above results show that the present method gives good estimation for both simulated data and experimental data. Moreover, the present estimation does not need a very long record. This will lead to less computation time, which is an important factor in an "on-line" processing program. This also means that it can open up the possibility of continuously monitoring all relevant ship roll parameters and displaying up-to-date information to the captain.

In a conventional way, to estimate all the parameters in the roll equation one needs two experimental runs. In the first run, the ship is restrained while excitation moment from waves is measured. Then the ship is set free and the response is measured. To obtain the relation between the input and output, the combined two sets of data are required. The difficulty of doing this is that it can not be insured that we have exactly the same condition in the two test runs. The present method allows us to estimate all the parameters in the roll equation in one experimental run.

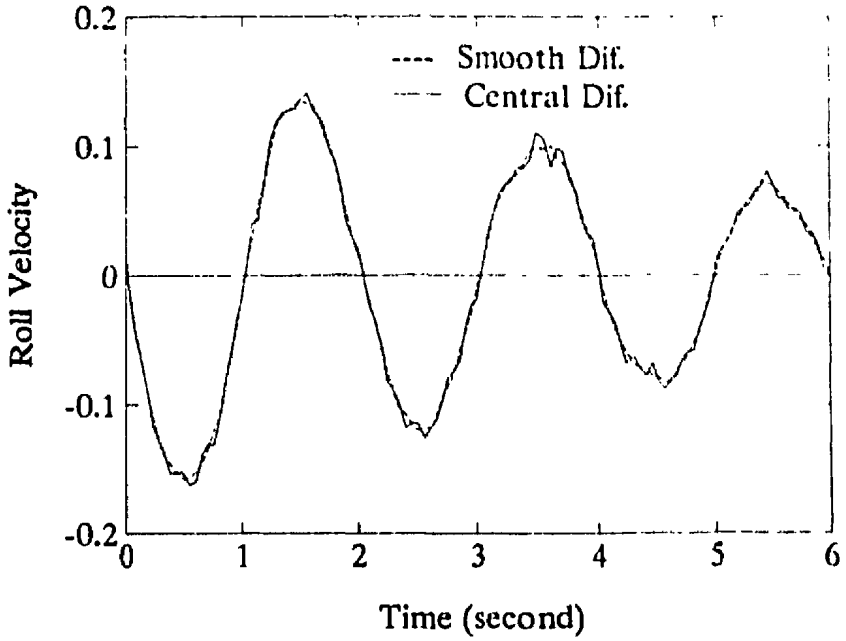

Figure 3.1: Comparison of two numerical difference formulas

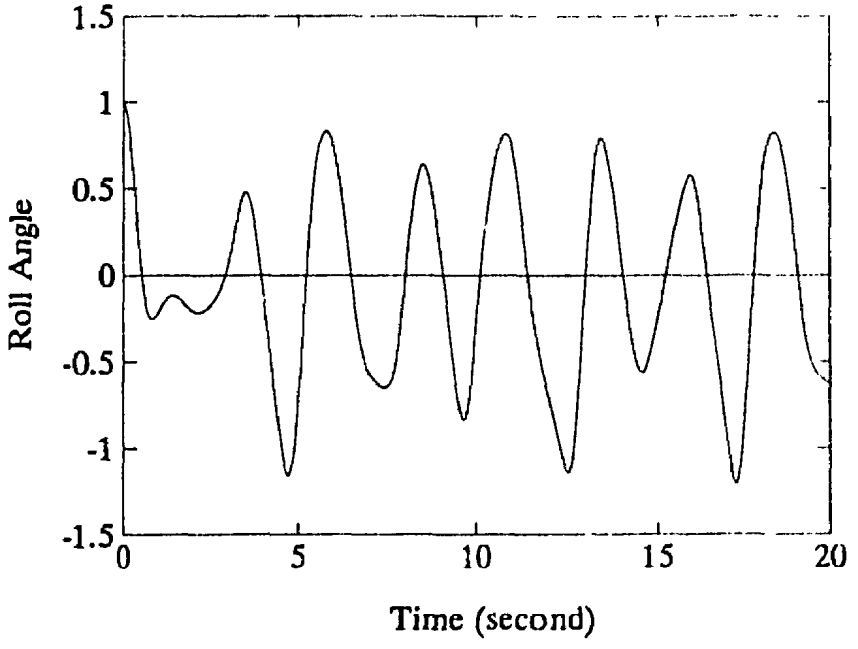

Figure 3.2: Simulated $\varphi(t)$ curve (Data set A)

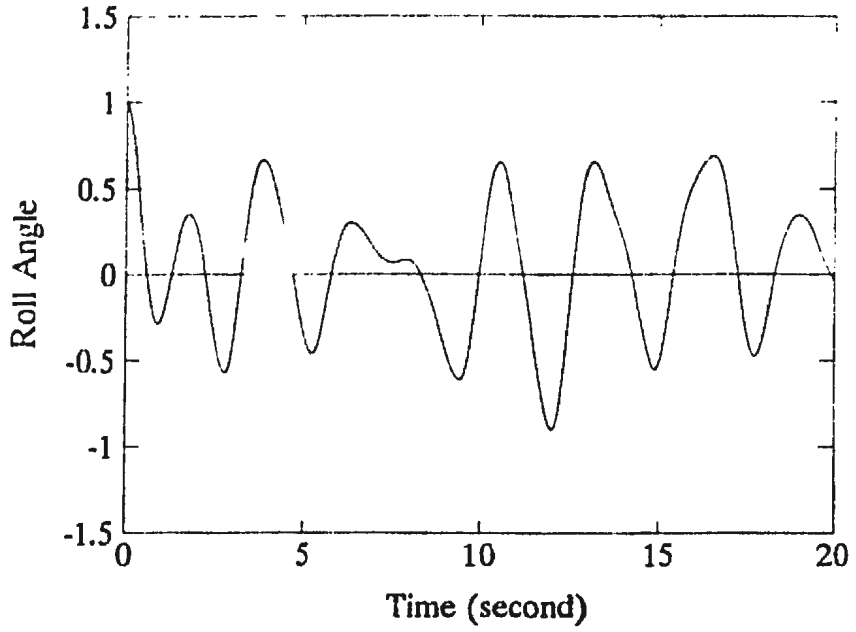

Figure 3.3: Simulated $\varphi(t)$ curve (Data set B)

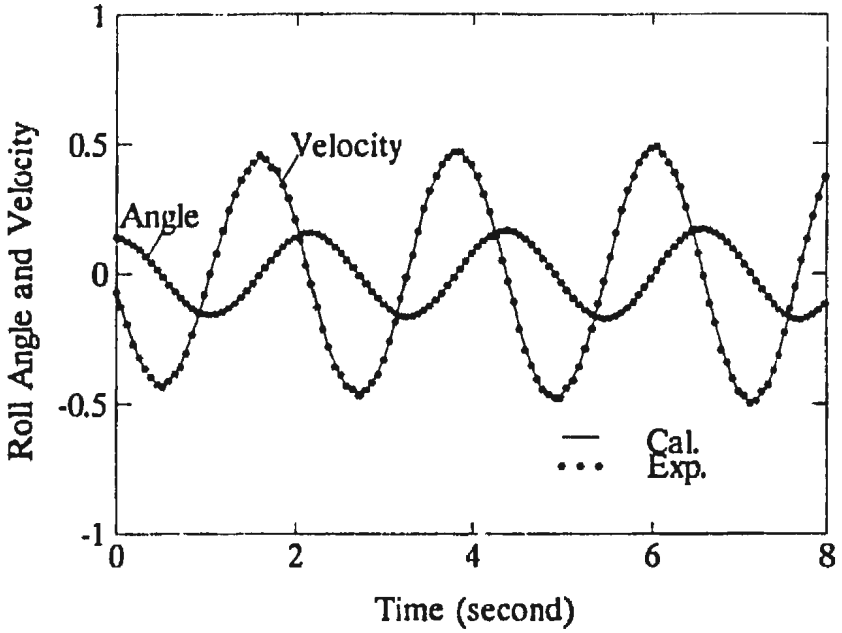

Figure 3.4: Comparison of experimental data and reproduced $\varphi(t)$curve of forced roll motion

Chapter 4

Estimation of Ship Roll Parameters from Free Roll Decay Curves

4.1 Analysis of Free Roll Decay Data

For the parametric identification from free roll decay data, the only problem is how to improve the accuracy of estimation. The work in this Chapter will show the viability and accuracy of the method mentioned in Chapter 2 for the parametric identification using free roll decay data. Moreover, the parameters estimated from the free roll decay data can be used as a comparison to the results estimated from the random roll data for the same ship model. From the analysis of experimental data, the relationship between the damping coefficients and the amplitude of roll motion, and the relationship between GM values (Metacentric height) and the linear natural frequency are obtained.

Letting the coefficients δ, K in equation (2.4) be zero, the governing equation of free roll motion can be written as:

$$\ddot{\varphi} + B_0\dot{\varphi} + B_1\dot{\varphi}|\dot{\varphi}| + A_0\varphi + A_1\varphi^3 + A_2\varphi^5 = 0 \qquad (4.1)$$

Table 4.1: Comparison between estimated and given parameters

Parameters	B_0	B_1	A_0	A_1	A_2
Given	0.20000	0.05000	10.00000	5.00000	3.00000
Estimated	0.20002	0.04999	10.00018	4.99997	3.00030

After applying the modulating function operation to equation (4.1), the roll parameters can be obtained from the following algebraic equations:

$$\overline{\Psi_{n+2}(\varphi)} + B_0\overline{\Psi_{n+1}(\varphi)} + B_1\Psi_n(\dot{\varphi}|\dot{\varphi}|) + A_0\Psi_n(\varphi) + A_1\Psi_n(\varphi^3) + A_2\Psi_n(\varphi^5)$$
$$= 0 \qquad (n = 0, 1, 2, 3, 4) \tag{4.2}$$

4.2 Examples and Results

4.2.1 Simulated Data

From the data obtained by numerical integration on equation (4.1) with some given parameters, the estimation of these parameters can be obtained by the present method. Table 4.1 shows a very good agreement between the given parameters and estimated ones.

4.2.2 Experimental Data

The experimental data is obtained from ship model tests in the wave tank at Memorial University of Newfoundland. These tests are carried out while the ship models have varied GM values and constant masses. The GM values are changed by moving the position of the center of gravity. More details about the ship model tests can be found in reference [12]. The ship models used in the tests are Model 363, 365 and 366. The information about these models is given in Appendix C.

Table 4.2: Parameters estimated for Model 363

GM	$InitialAngle$	B_0	B_1	A_0	A_1	A_2
3.81	5.29	0.09222	0.00082	7.95503	-4.18495	-0.16614
3.81	9.10	0.10241	0.00704	8.07450	-4.67637	-0.18565
3.81	11.68	0.12617	0.00636	7.95503	1.26963	0.05040
3.81	14.48	0.16615	0.00734	8.09178	-1.11603	-0.04431
3.81	17.35	0.15339	0.00941	8.19669	-0.23518	-0.00934
3.81	-6.20	0.07548	0.01254	7.95503	-11.49091	-0.45619
3.81	-9.53	0.10630	0.03266	8.07450	-2.64188	-0.10488
3.81	-11.13	0.11113	0.03016	7.98889	-1.15493	-0.04585
3.81	-14.59	0.14763	0.00419	8.19669	-1.27408	-0.05058
3.81	-17.26	0.15348	0.00104	8.19669	-0.69947	-0.02777
3.10	3.76	0.15260	0.01509	7.39584	18.35989	1.59547
3.10	6.67	0.22587	0.00648	7.50284	-1.24522	-0.10821
3.10	9.67	0.27992	0.00728	7.50284	1.60828	0.13976
3.10	12.33	0.32414	0.02644	7.61218	-6.33183	-0.55024
3.10	3.80	0.17117	0.01801	7.61218	-46.89713	-4.07536
3.10	-4.70	0.20942	0.00716	7.61218	-1.17260	-0.10190
3.10	-4.75	0.20038	0.00742	7.50284	-9.18292	-0.79800
3.10	-10.10	0.27492	0.04291	7.50284	-12.48622	-1.08505
3.10	-13.29	0.33421	0.03276	7.61318	-3.37972	-0.29370
3.10	-16.89	0.34245	0.06881	7.50284	-1.12257	-0.09755
2.51	4.31	0.23447	0.00581	4.96678	-83.80376	-12.27725
2.51	7.45	0.33619	0.00407	4.93466	-9.57852	-1.40325
2.51	9.63	0.38084	0.01874	4.86645	-7.43730	-1.08956
2.51	13.19	0.44143	0.00232	4.93466	-11.51711	-1.68726
2.51	17.02	0.51126	0.04270	4.93466	-1.84884	-0.27086
2.51	-4.52	0.23193	0.03935	4.86645	-4.60779	-0.67504
2.51	-7.16	0.32367	0.02999	4.86645	-4.53998	-0.66511
2.51	-10.30	0.41464	0.00376	4.86645	-19.58479	-2.86917
2.51	-13.99	0.42565	0.01039	4.93466	-18.00570	-2.63784
2.51	-17.22	0.51793	0.03937	4.86645	-6.29363	-0.92202

Table 4.3: Parameters estimated for Model 365: First part

GM	$InitialAngle$	B_0	B_1	A_0	A_1	A_2
4.31	8.73	0.17965	0.00283	12.96544	2.66977	-0.68079
4.31	10.04	0.18785	0.00243	12.87315	0.56228	-0.14338
4.31	11.53	0.22226	0.00729	12.87316	8.17754	-2.08527
4.31	13.09	0.23884	0.00429	12.87316	-5.76293	1.46955
4.31	17.87	0.33512	0.00373	12.87316	13.78113	-3.51419
4.31	-9.02	0.19707	0.00229	13.10574	-22.49528	5.73630
4.31	-11.71	0.27018	0.00522	12.87315	2.06812	-0.52737
4.31	-13.96	0.22018	0.00980	12.87315	-2.94864	0.75190
4.31	-16.39	0.30974	0.00939	12.87315	-5.87162	1.49726
4.31	-20.34	0.33879	0.00850	12.87315	-6.14638	1.56733
3.61	7.02	0.17658	0.00600	11.59953	-4.89199	1.33062
3.61	10.42	0.22491	0.00442	11.59953	-6.88459	1.87261
3.61	12.51	0.25527	0.00324	11.44414	1.17918	-0.32074
3.61	15.24	0.31754	0.00437	11.59953	-9.15257	2.48950
3.61	19.30	0.30045	0.00936	11.59953	4.41370	-1.20053
3.61	-9.93	0.18589	0.00922	11.40578	5.09182	-1.38498
3.61	-13.17	0.24773	0.00770	11.40578	-0.73706	0.20048
3.61	-16.44	0.33494	0.00486	11.59953	15.16715	-4.12546
3.61	-19.51	0.32476	0.00785	11.40578	-3.72252	1.01253
3.61	-24.81	0.37223	0.00891	11.21685	0.33544	-0.09124
3.26	11.40	0.21760	0.00375	10.78216	-14.62094	4.13773
3.26	12.30	0.24855	0.00164	10.57424	-3.18194	0.90049
3.26	15.15	0.33482	0.00237	10.57425	9.73226	-2.75423
3.26	19.80	0.34480	0.00526	10.37231	0.96148	-0.27210
3.26	24.06	0.38444	0.00513	10.37230	-2.27489	0.64379
3.26	-10.22	0.19700	0.00205	10.57424	-0.78272	0.22151
3.26	-14.99	0.30068	0.00530	10.57425	-9.35908	2.64862
3.26	-16.10	0.29903	0.00368	10.57425	-4.27038	1.20852
3.26	-21.39	0.35080	0.00613	10.37231	-0.77780	0.22012
3.26	-27.49	0.39295	0.00644	10.17610	0.83863	-0.23733

Table 4.4: Parameters estimated for Model 365: Second part

GM	$InitialAngle$	B_0	B_1	A_0	A_1	A_2
2.75	9.88	0.20364	0.00190	8.94657	-3.54436	1.08103
2.75	15.40	0.29038	0.00438	8.78932	1.97330	-0.60186
2.75	15.63	0.30361	0.00110	8.94656	-5.79450	1.76732
2.75	17.72	0.32438	0.00047	8.78932	0.56385	-0.17197
2.75	29.01	0.37298	0.00952	8.63619	-1.62342	0.49514
2.75	-11.77	0.22089	0.00015	8.94657	-6.21391	1.89524
2.75	-14.08	0.25677	0.01781	8.94656	-7.17096	2.18714
2.75	-19.14	0.30960	0.00384	8.78932	-2.06362	0.62940
2.75	-21.81	0.33533	0.00964	8.63619	1.06741	-0.32556
2.75	-25.53	0.36580	0.00828	8.63619	-0.00293	0.00089
2.39	9.58	0.18264	0.00716	7.66839	-9.52594	3.11498
2.39	13.70	0.24388	0.00034	7.48229	0.40787	-0.13337
2.39	14.72	0.27573	0.00052	7.66839	-21.23252	6.94303
2.39	17.51	0.28078	0.04286	7.54365	2.76427	-0.90392
2.39	22.12	0.32963	0.00304	7.54356	-5.29641	1.73193
2.39	-10.60	0.21592	0.00958	7.66839	-4.85985	1.58917
2.39	-14.08	0.26331	0.00590	7.63689	-3.05489	0.99895
2.39	-17.62	0.31890	0.00877	7.54356	-0.62392	0.20402
2.39	-18.79	0.33297	0.00533	7.48229	0.93011	-0.30415
2.39	-24.13	0.36268	0.00181	7.33235	0.43515	-0.14229

Table 4.5: Parameters estimated for Model 366: First part

GM	$InitialAngle$	B_0	B_1	A_0	A_1	A_2
5.29	21.42	0.26021	0.00506	12.01970	-0.96070	0.01739
5.29	26.80	0.31014	0.01480	12.01968	-0.30991	0.00561
5.29	-6.73	0.10121	0.00837	12.01968	-9.24717	0.16737
5.29	-11.17	0.14490	0.00698	12.18665	-17.09653	0.30945
5.29	-15.43	0.18455	0.00024	11.81578	2.19304	-0.03969
5.29	-20.14	0.23614	0.00376	11.81578	4.27914	-0.07745
5.29	-23.89	0.29464	0.00261	12.01968	-2.14368	0.03880
5.29	10.98	0.13861	0.00148	11.81578	2.85178	-0.05162
5.29	15.74	0.16989	0.01007	11.81577	1.69434	-0.03067
5.29	19.17	0.25091	0.01430	12.22893	-9.12100	0.16509
4.91	25.83	0.30985	0.00306	11.46164	-1.64868	0.01088
4.91	24.93	0.29630	0.00775	11.42328	-1.86648	0.01232
4.91	-8.46	0.12011	0.01664	11.21685	9.10805	-0.06011
4.91	-11.36	0.14603	0.00621	11.23435	5.18992	-0.03425
4.91	-14.77	0.16761	0.01535	11.23435	4.37853	-0.02890
4.91	-21.33	0.24510	0.00207	11.23435	2.54312	-0.01678
4.91	-27.80	0.31594	0.00186	11.42328	-0.49546	0.00327
4.91	12.16	0.14375	0.00554	11.42328	-4.08950	0.02699
4.91	13.23	0.15583	0.00165	11.23435	3.61592	-0.02387
4.91	20.23	0.23558	0.00704	11.23435	1.18446	-0.00782

Table 4.6: Parameters estimated for Model 366: Second part

GM	$InitialAngle$	B_0	B_1	A_0	A_1	A_2
3.92	25.27	0.27967	0.02086	9.12558	1.13138	0.03824
3.92	28.31	0.30839	0.00237	9.29153	-1.79792	-0.06077
3.92	-6.66	0.10148	0.01144	9.29153	-19.52801	-0.66005
3.92	-9.71	0.12970	0.00002	9.12559	-1.51477	-0.05120
3.92	-17.24	0.21235	0.00999	9.12558	-0.22185	-0.00750
3.92	-18.57	0.23258	0.00068	9.12558	0.53163	0.01797
3.92	-26.81	0.30102	0.00357	9.29153	6.06672	0.20506
3.92	8.64	0.13348	0.04624	9.12559	-6.79987	-0.22984
3.92	14.40	0.18280	0.02483	9.12558	-2.23935	-0.07569
3.92	18.81	0.24906	0.00456	9.29153	-4.34618	-0.14690
3.38	22.76	0.24411	0.00525	7.65439	0.88590	0.05838
3.38	29.06	0.32273	0.00336	7.81385	-0.95438	-0.06289
3.38	-10.69	0.13112	0.00231	7.65439	2.77916	0.18315
3.38	-12.35	0.13911	0.03333	7.65439	1.34339	0.08853
3.38	-17.55	0.18829	0.06357	7.81385	-3.10143	-0.20438
3.38	-20.02	0.21753	0.00062	7.81385	-3.64426	-0.24016
3.38	-25.47	0.30288	0.02275	7.81385	-2.35469	-0.15517
3.38	12.39	0.14097	0.04031	7.81385	-7.43295	-0.48983
3.38	13.16	0.12797	0.00960	7.65439	-3.20950	-0.21151
3.38	21.52	0.22641	0.08064	7.97837	-5.39630	-0.35562

Generally, the measured data within 2 - 3 roll cycles are enough for the parameters estimation. Tables 4.2 - 4.6 give the estimated parameters for different GM values for the three ship models.

Using these estimated parameters, the curves of roll angle and its velocity are reproduced by numerical integration of equation (4.1). Figures 4.1 -4.3 show very good agreement between reproduced curves (solid line) and experimental ones (star marks) for the three ship models.

4.3 Discussion

From the physical assumption, the parameter A_0 in the roll equation is approximately a linear function of GM value given by

$$A_0 = \frac{\Delta GM}{I} \tag{4.3}$$

where I is the virtual mass moment of inertia of the ship about a longitudinal axis passing through the center of gravity of the ship and Δ is displacement.

From the estimated results, the values of A_0 were plotted against the GM values in Figures 4.4 - 4.6. The linear regression curves of these points are also given. For Models 365 and 366, the results show a perfect linear relationship. For Model 363, this linear relationship is not so obvious. This point needs to be investigated.

In Figures 4.7 - 4.9, the damping parameters B_0 are plotted against the initial angle of inclination for each model. It shows a linear relationship as indicated by the linear regression curves of the points. In Figure 4.8, it shows relatively large scatters in the data points in the area of roll angle whthin 15 to 20 degrees. The reason may be due to the "trade-offs" between linear and nonlinear damping parameters. Figure 4.7 shows that the linear damping coefficient B_0 is sensitive to the variation in GM value of the model. However, the effect of GM values on B_0 is minor for models 365 and 366 as seen from Figures 4.8 and 4.9.

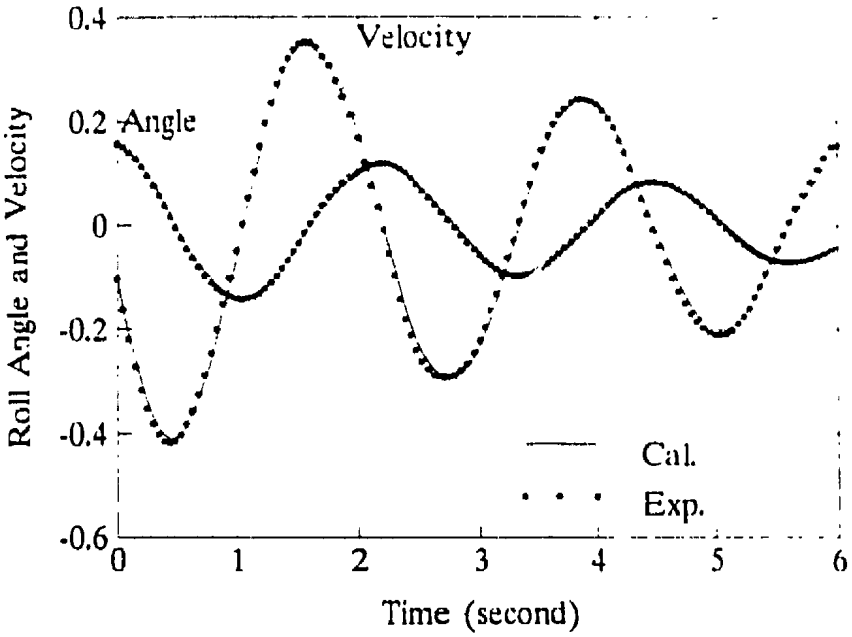

Figure 4.1: Comparison of estimated and experimental roll curves for Model 363

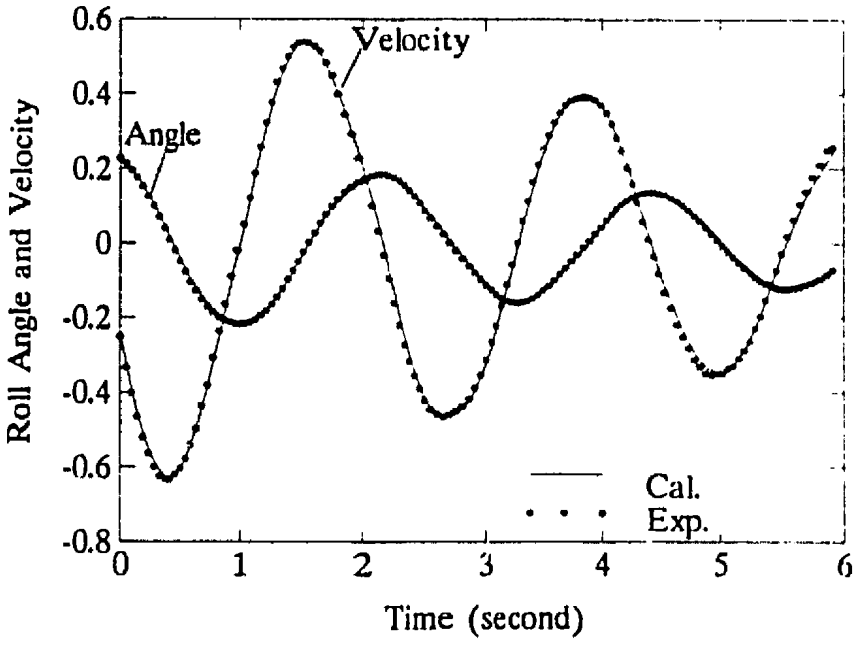

Figure 4.2: Comparison of estimated and experimental roll curves for Model 365

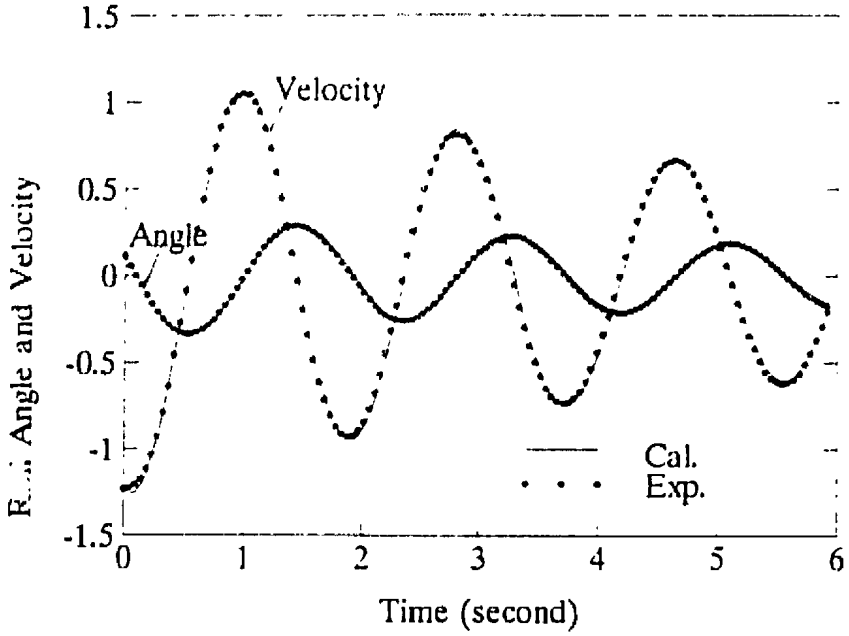

Figure 4.3: Comparison of estimated and experimental roll curves for Model 366

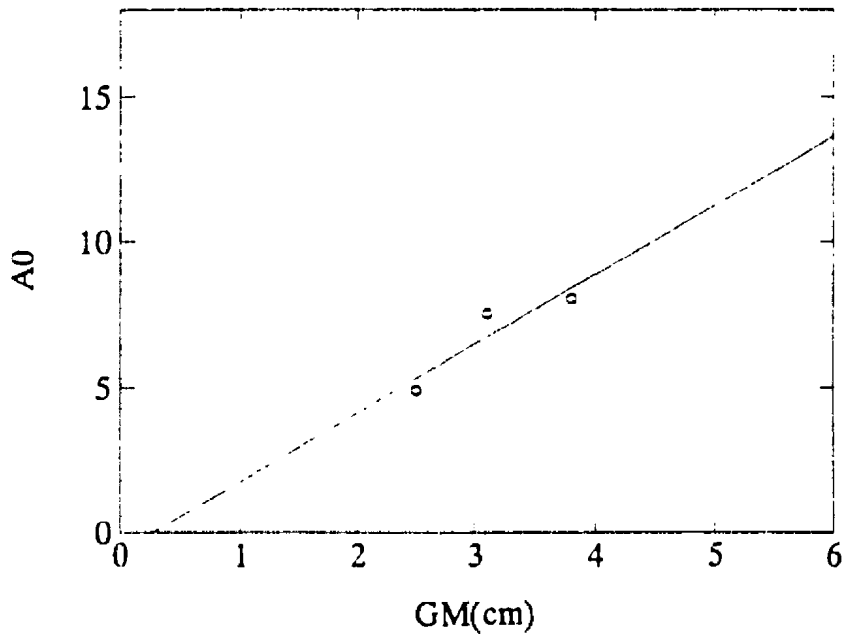

Figure 4.4: A_0 vs. GM of Model 363

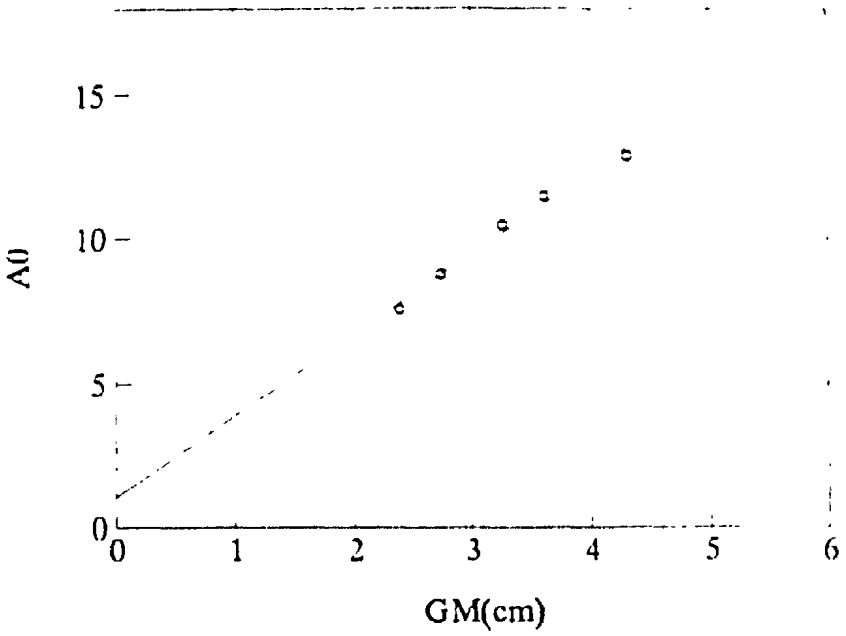

Figure 4.5: A_0 vs. GM of Model 365

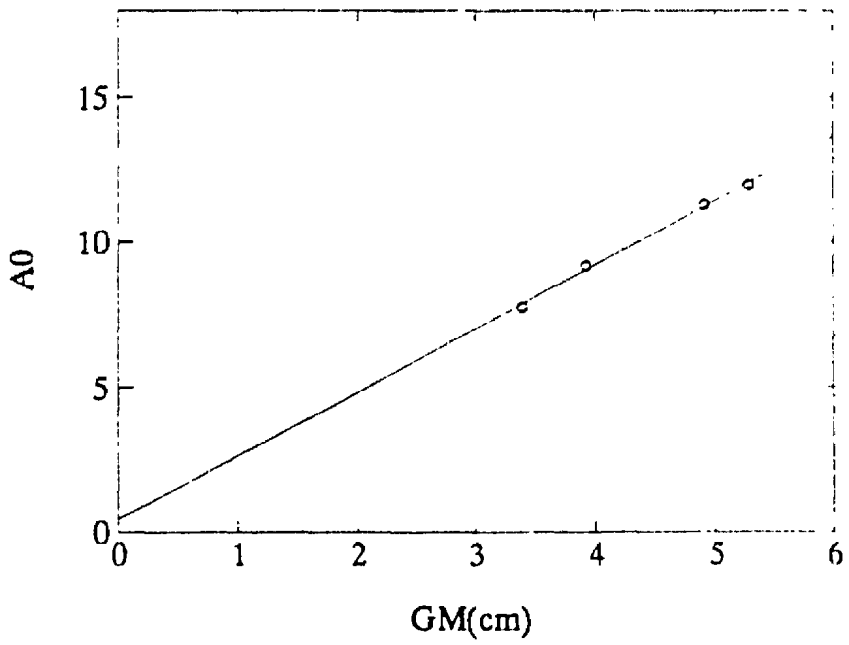

Figure 4.6: A_0 vs. GM of Model 366

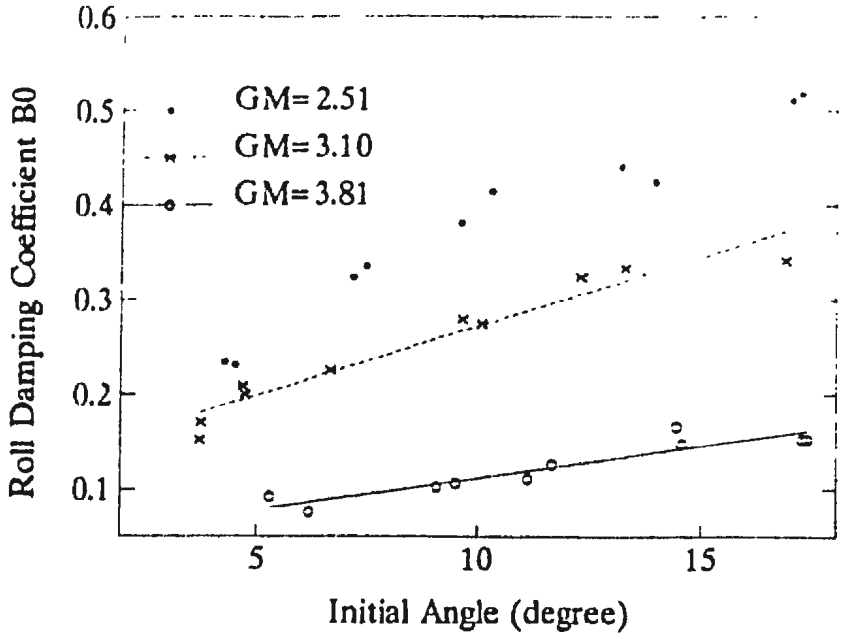

Figure 4.7: Roll damping vs. initial angle for different GM values (Model 363)

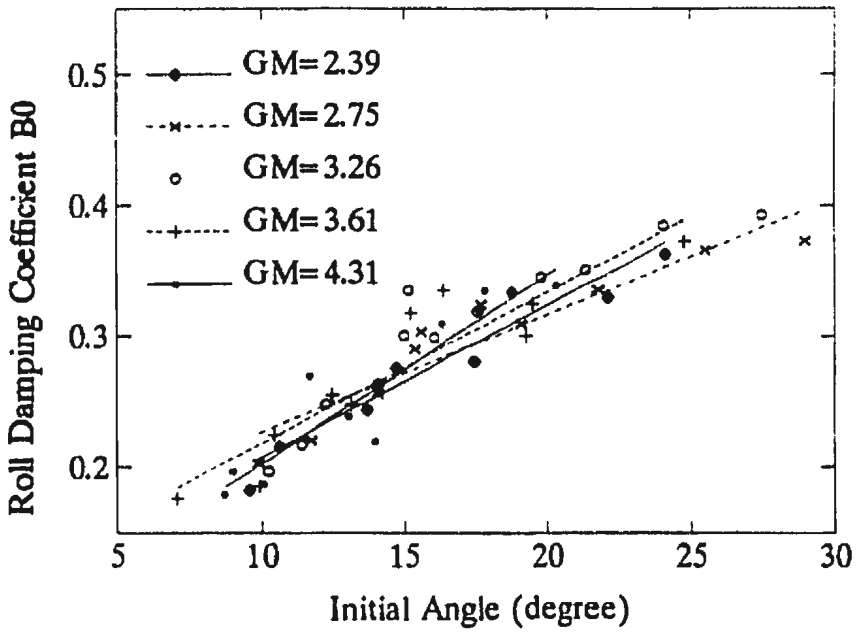

Figure 4.8: Roll damping vs. initial angle for different GM values (Model 365)

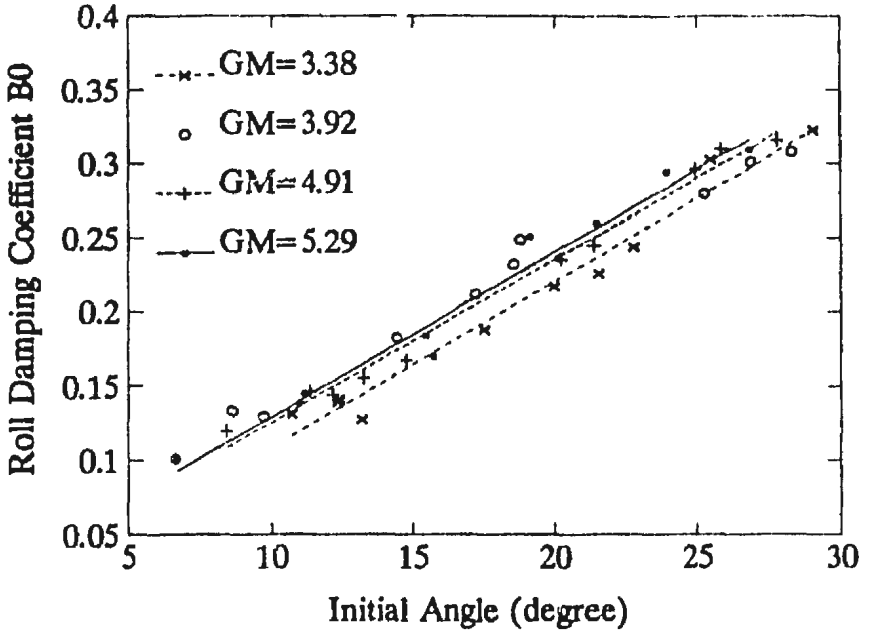

Figure 4.9: Roll damping vs. initial angle for different GM values (Model 366)

Chapter 5

Estimation of Ship Roll Parameters from Roll Response in Random Waves

5.1 Introduction

The ship roll parameters will change when the ship loading changes. It is very important to be able to apply the parametric identification method to real ship responses at sea. A new approach to estimate the ship roll parameters in random waves is discussed in this Chapter.

In order to apply our parametric identification method to this problem, the equation for the autocorrelation or random decrement of roll angle was derived to replace the original roll equation. The derived equation has a similar form as the original roll equation. From the equation of autocorrelation or random decrement, the roll parameters can be estimated using the method discussed in Chapter 3.

Reference [10] provides a method based on the Markov property of energy envelope process to estimate roll parameters with the assumption that the excitation is a white noise. No attempt has been made to apply this method to experimental

data. In our method, the assumption of white noise excitation is not necessary. In order to test the form of excitation moment and the crosscorrelation between excitation moment and the roll response, two different excitation moments are used in the present study. The first one is a random process uncorrelated with the roll response. The second one is a narrow-band process given by a second-order linear differential equation. The results show that the narrow-band excitation moment will correlate with the roll response but this correlation is relatively weak.

The method was first applied to a set of numerically simulated roll data, for which the true parameters are known. The estimated parameters show a good agreement with the true parameters. The second test case is to apply this method to the measured roll data obtained from the ship model test in random waves. Using the estimated parameters, the autocorrelation or decrement curves were reproduced by numerical integration. They also show a good agreement with the relevant curves calculated from the experimental data.

As expected, the damping and stiffness parameters estimated from the random roll motion are very close to the results obtained from the free roll decay test for the same ship model.

Since the present method only depends on the measured roll data, it is possible to apply it to full scale ships at sea. The last test case is to use this method to analyse the measured roll data of a full scale ship at sea. Although the measured data of the real ship are much more noisy than the experimental data of the ship model, the estimation also gives reasonably good results.

5.2 Parametric Identification

The roll motion of a ship subjected to a roll excitation moment $M(t)$ is written as:

$$\ddot{\varphi} + B_0\dot{\varphi} + B_1\dot{\varphi}|\dot{\varphi}| + A_0\varphi + A_1\varphi^3 + A_2\varphi^5 = KM(t) \tag{5.1}$$

Equation (5.1) can be considered as a single input-output system. Because only measured roll response is available while input $M(t)$ is very difficult to be obtained, we can not estimate parameters from equation (5.1) directly. To solve this problem, two approaches are discussed.

5.2.1 Autocorrelation Equation

Assuming the roll response is a stationary process, the autocorrelation of roll angle is defined as:

$$R(\tau) = < \varphi(t)\varphi(t+\tau) > \tag{5.2}$$

where $<\quad>$ means ensemble average on time t.

Differentiating $R(\tau)$ about τ and introducing equation (5.1) gives

$$\dot{R}(\tau) = < \varphi(t)\dot{\varphi}(t+\tau) > \tag{5.3}$$

$$\begin{aligned}\ddot{R}(\tau) &= < \varphi(t)\ddot{\varphi}(t+\tau) > \\ &= K < \varphi(t)M(t+\tau) > -B_0 < \varphi(t)\dot{\varphi}(t+\tau) > \\ &\quad -B_1 < \varphi(t)\dot{\varphi}(t+\tau)|\dot{\varphi}(t+\tau)| > -A_0 < \varphi(t)\varphi(t+\tau) > \\ &\quad -A_1 < \varphi(t)\varphi^3(t+\tau) > -A_2 < \varphi(t)\varphi^5(t+\tau) >\end{aligned} \tag{5.4}$$

Combining the above equations, an autocorrelation equation of roll angle is obtained as:

$$\ddot{R}(\tau) + B_0\dot{R}(\tau) + A_0R(\tau) + B_1f_1(\tau) + A_1g_1(\tau) + A_2h_1(\tau) = Ke_1(\tau) \qquad (5.5)$$

where

$$f_1(\tau) =< \varphi(t)\dot{\varphi}(t+\tau)|\dot{\varphi}(t+\tau)| > \qquad (5.6)$$

$$g_1(\tau) =< \varphi(t)\varphi^3(t+\tau) > \qquad (5.7)$$

$$h_1(\tau) =< \varphi(t)\varphi^5(t+\tau) > \qquad (5.8)$$

$$e_1(\tau) =< \varphi(t)M'(t+\tau) > \qquad (5.9)$$

5.2.2 Equation for the Random Decrement

The random decrement operation is the average of some selected segments of records. These segments have the same length and the same initial value. For example, the random decrement of roll angle $\varphi(\tau)$ can be expressed as:

$$< \varphi(\tau) >= \frac{1}{N}\sum_{i=1}^{N}\varphi_i(\tau) \qquad 0 \le \tau \le \tau_{max} \qquad (5.10)$$

where $<\ >$ means an ensemble average of the process.

Performing such operation on equation (5.1) results in the following equation:

$$\ddot{\mu}(\tau) + B_0\dot{\mu}(\tau) + A_0\mu(\tau) + B_1 < \dot{\varphi}|\dot{\varphi}| > + A_1 < \varphi^3 > + A_2 < \varphi^5 >$$
$$= K < M(\tau) > \qquad (5.11)$$

where $\mu(\tau) =< \varphi(\tau) >$.

More details about how to calculate random decrement from random responses can be found in references [11] and [20].

For convenience, Equations (5.5) and (5.11) can be written in a uniform form:

$$\ddot{Y}_i(\tau) + B_0\dot{Y}_i(\tau) + A_0Y_i(\tau) + B_1f_i(\tau) + A_1g_i(\tau) + A_2h_i(\tau)$$
$$= Ke_i(\tau) \qquad (i = 1, 2) \tag{5.12}$$

For autocorrelation equation, $i = 1$:

$$Y_1(\tau) = R(\tau)$$
$$f_1(\tau) = < \varphi(t)\dot{\varphi}(t+\tau)|\dot{\varphi}(t+\tau)| >$$
$$g_1(\tau) = < \varphi(t)\varphi^3(t+\tau) >$$
$$h_1(\tau) = < \varphi(t)\varphi^5(t+\tau) >$$
$$e_1(\tau) = < \varphi(t)M(t+\tau) >$$

For random decrement equation, $i = 2$:

$$Y_2(\tau) = \mu(\tau)$$
$$f_2(\tau) = < \dot{\varphi}(\tau)|\dot{\varphi}(\tau)| >$$
$$g_2(\tau) = < \varphi^3(\tau) >$$
$$h_2(\tau) = < \varphi^5(\tau) >$$
$$e_2(\tau) = < M(\tau) >$$

If $M(t)$ is uncorrelated with $\varphi(t)$, then $e_1(\tau)$ is equal to zero in the autocorrelation equation, the parameters can be estimated without knowing the excitation. Some researchers consider this assumption acceptable or assume $M(t)$ to be a white noise. In this thesis, this assumption will be tested by numerical simulation.

As the wave exciting moment is a narrow-band process, it can be described approximately by the following equation:

$$\ddot{M}(t) + \gamma\dot{M}(t) + \omega^2 M(t) = u(t) \tag{5.13}$$

where γ is the band width and ω is the central frequency of this process. $u(t)$ is a white noise with unit variance.

The solution of equation (5.13) was used as excitation moment in our study.

5.2.3 Modulating Function Operation

Applying the modulating function operation on equation (5.12) and letting n be from 0 to $L-1$, (where L is the number of unknown parameters), a set of algebraic equations for the unknown parameters can be obtained as:

$$\begin{aligned} &T_r^2\Psi_{n+2}(Y_i) + B_0T_r\Psi_{n+1}(Y_i) + A_0\Psi_n(Y_i) + B_1\Psi_n(f_i) + A_1\Psi_n(g_i) + A_2\Psi_n(h_i) \\ &= K\Psi_n(e_i) \qquad (i = 1,2) \\ &\qquad (n = 0, 1, \ \ldots. \ L-1) \end{aligned} \tag{5.14}$$

To make the problem simple, $T_s = T_e = T_\infty$ is used.

From this equation, values for the roll parameters can be solved.

5.3 Examples and Results

5.3.1 Simulated Data

The use of simulated data to validate a method has some advantages. For example, the values of the test parameters are known in advance. This allows a

Table 5.1: Estimated parameters and their true values
$\omega = 3.0 \quad \gamma = 0.5$

Para.	B_0	B_1	A_0	A_1	A_2	K
Given	0.10000	0.10000	9.00000	1.00000	0.00000	10.00000
Esti.(A)	0.09869	0.10296	9.09674	0.87521	0.00000	10.10105
Esti.(B)	0.10249	0.09711	9.05609	0.88799	0.00000	9.70994
Esti.(C)	0.10595	0.09628	9.00056	1.13665	0.00000	10.15320

direct comparison between the estimated parameters and their true values. Secondly, the duration of the samples can be chosen arbitrarily to show its effects on the estimation process.

To generate roll motion samples with a random excitation, equation (5.1) was integrated numerically with given parameters. In the time length of 400 seconds, 16001 data of roll angle are picked with a equal time interval. $M(t)$ is the solution of equation (5.13) and $u(t)$ is a white noise which can be generated from a sequence of independent Gaussian random numbers.

The solution $\varphi(t)$ was used to calculate the autocorrelation, crosscorrelation and random decrement in equation (5.12), from this equation the parameters can be estimated. Table 5.1 shows a comparison between the estimated values of the parameters and their true values. Three sets of test results are reported here: sets A and B are estimated from correlation having a length of 5 seconds and 10 seconds, respectively. All correlation is calculated from roll samples having a length of 400 seconds. Set C is the result estimated from the same data in set B using the random decrement equation. The results show very good agreement for all cases. It can also be noticed that there are some 'trade-offs' between B_0, B_1 and A_0, A_1, A_2.

Figure 5.1 shows the variations of roll moment and roll response with time. Both roll moment and response are in the practical range. Figure 5.2 shows the spectral density of roll moment and roll response.

5.3.2 Experimental Data

The second test case is to use this method to analyse the experimental data. The experimental data are obtained from model tests in the towing tank of Memorial University of Newfondland on three fishing vessels. Both free roll and randomly excited roll are measured. The random waves are generated by JONSWAP spectrum.

The ship models are Model 363, 365 and 366. The particulars of these models can be found in Appendix C. As an example, we focus on the analysis of the experimental data on model 366.

A total of 8001 samples of roll angle with a uniform time interval of $(\frac{1}{21})$ second were used to calculate the correlation and the random decrement. Four cases are considered:

(A) using autocorrelation equation. $M(t)$ is a narrow-band process with a central frequency ω of 3.2 (rad/sec) and a band width γ of 0.2.

(B) using autocorrelation equation. $M(t)$ is assumed to be uncorrelated with the roll response, that is, $e_1(\tau) = 0$.

(C) using random decrement equation.

(D) estimation from free roll data.

The estimated parameters are listed in Table 5.2. The Table shows that the results in different cases are very close to each other. K is the amplitude of the

Table 5.2: Estimated parameters of Model 366 (GM=4.91cm)

Para.	B_0	B_1	A_0	A_1	A_2	K
A	0.12018	0.00361	11.39600	1.34132	-0.00832	0.22097
B	0.11933	0.00446	11.39600	1.33536	-0.00828	—
C	0.11496	0.00268	11.44414	2.23575	-0.01386	0.20912
D	0.12011	0.01664	11.21685	9.10805	-0.05647	—

excitation. Because there are 'trade-offs' between parameters, it is not easy to see the difference between the different estimation. An alternative way of judgement is to make an overall comparison, i.e., to integrate the free roll equation with estimated parameters A_0, A_1, A_2, B_0, B_1 of different cases and then to compare integrated roll curves. Figure 5.3 shows such a comparison. Because the results in case A and B are almost the same, only three integration curves are ploted for case A, C and D. The results indicate that the estimation obtained from the autocorrelation equation or from the random decrement equation are very close to the results obtained from free roll decay test in general. That is just what we expected. That means it is possible to apply this method for the parametric estimation from the response of a ship at sea instead of from a free roll decay test. It can also be noticed that the crosscorrelation between the excitation and response can be omited. Figure 5.4 shows the comparison of the magnitudes of autocorrelation and crosscorrelation ($A_0R(t)$ *vs.* $Ke_1(t)$).

Using estimated parameters, the curves of autocorrelation $R(\tau)$ and roll angle $\varphi(t)$ as well as their derivatives were reproduced by numerical integration. Figures 5.5 to 5.7 show the comparisons between the reproduced curves and the curves obtained from experimental data for cases A, C and D. The star marks represent the experimental data while the solid lines represent the estimated values. The

Table 5.3: Estimated parameters of Model 365 (GM=4.31cm)

Para.	B_0	B_1	A_0	A_1	A_2	K
A	0.18699	0.02699	12.54371	-0.90693	0.22952	0.25931
C	0.18653	0.04548	12.42621	-1.09992	0.28048	0.25899
D	0.18702	0.02682	12.87316	-1.16877	0.29804	---

Table 5.4: Estimated parameters of Model 363 (GM=3.10cm)

Para.	B_0	B_1	A_0	A_1	A_2	K
A	0.18668	0.02053	7.20389	-15.85033	-0.04293	0.08204
C	0.17892	0.04002	7.07639	-18.61688	-1.22499	0.08031
D	0.18466	0.02516	7.55026	-15.90525	-1.06829	- -

results show a good agreement.

From the test data of the other two ship models, the roll parameters are also estimated and shown in Table 5.3 and 5.4. There are also good agreement between the parameters estimated from the free roll data and that from the random roll data.

5.3.3 Full Scale Ship Roll Data

More convincing way to test a method is to apply it to a practical situation. For this purpose, the roll data of a full scale fishing vessel obtained during a fishing trip was recorded and analysed using the present method. Because of the complex wave pattern and ship motion at sea, the measured roll data of this case seem much more noisy than the experimental data. However, the autocorrelation extracted from the measured data are still very smooth curves. From these autocorrelation curves, the roll parameters are estimated and shown in Table 5.5.

Table 5.5: Estimated parameters about full scale ship

Para.	$GM(m)$	B_0	B_1	A_0	A_1	A_2	K
A	0.6989	0.08716	0.00277	0.55145	-2.97636	-1.88832	0.01761
B	0.7091	0.08399	0.00870	0.57735	-3.82195	-1.90828	0.02191
C	0.7287	0.08072	0.00219	0.59571	-2.23287	-1.12686	0.02214

The data of three loading conditions of the ship in the same trip are analysed. The GM values of different loading conditions can also be estimated from hydrostatic calculations [12], which are also included in this Table. Figure 5.8 shows a approximate linear relationship between GM values and A_0 (the square of linear natural frequency).

Figures 5.9 to 5.11 show the fitness between the autocorrelation calculated from the experimental data and from the data of numerical integration on autocorrelation equation with estimated parameters.

The comparison between estimated data and experimental or simulated data indicates that:

(1) it is possible to estimate ship roll parameters from measured random roll responses only.

(2) the present method gives a fairly accurate estimation.

(3) the crosscorrelation between excitation and response can be neglected.

(4) the estimation from random roll motion gives very close results to that obtained from free roll decay tests, therefore, it is possible to use this method to estimate roll parameters from the random response of a ship at sea.

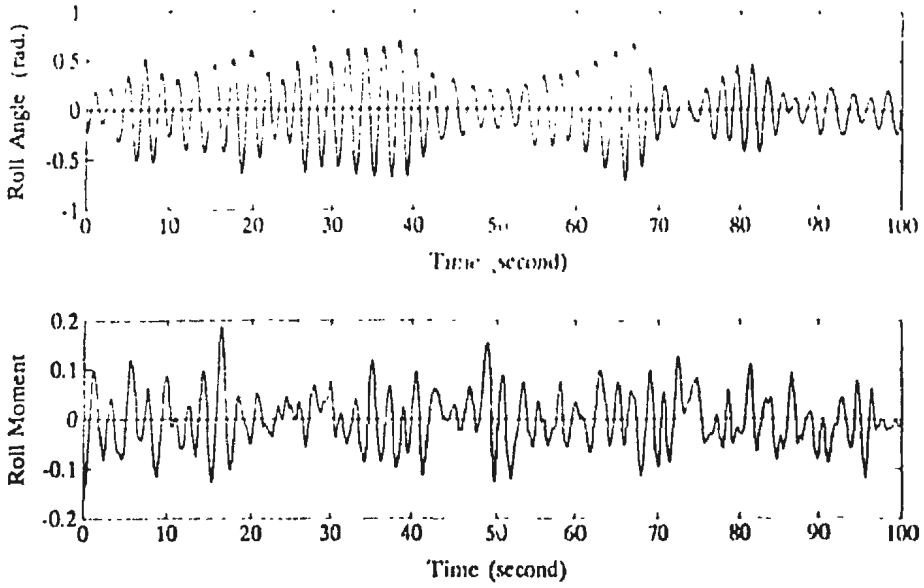

Figure 5.1: Variations of roll moment and roll response for simulated data

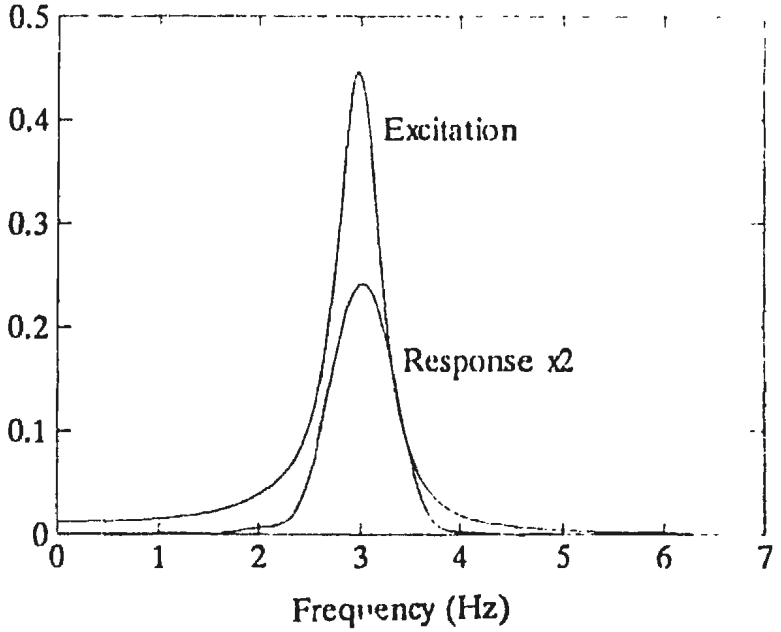

Figure 5.2: Spectrum of roll moment and roll response for simulated data

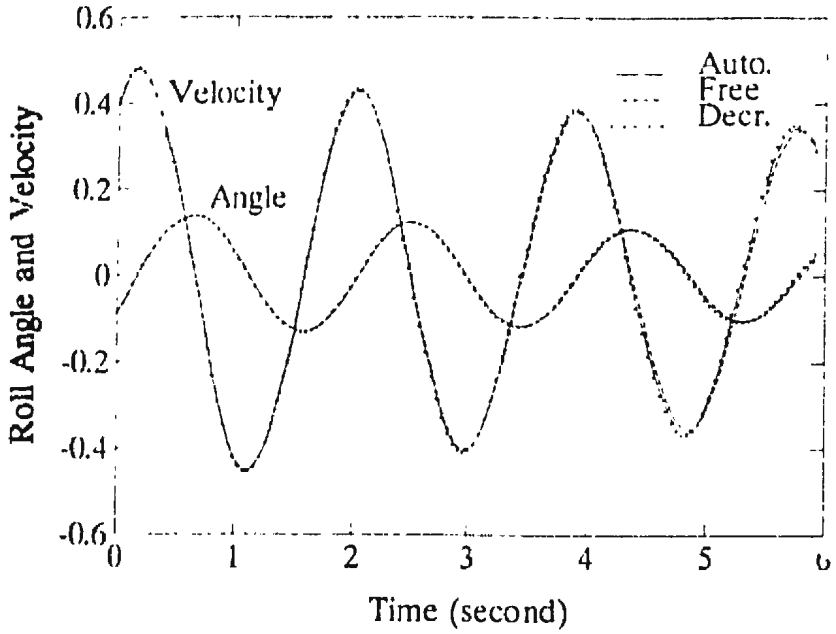

Figure 5.3: Comparison between different estimation

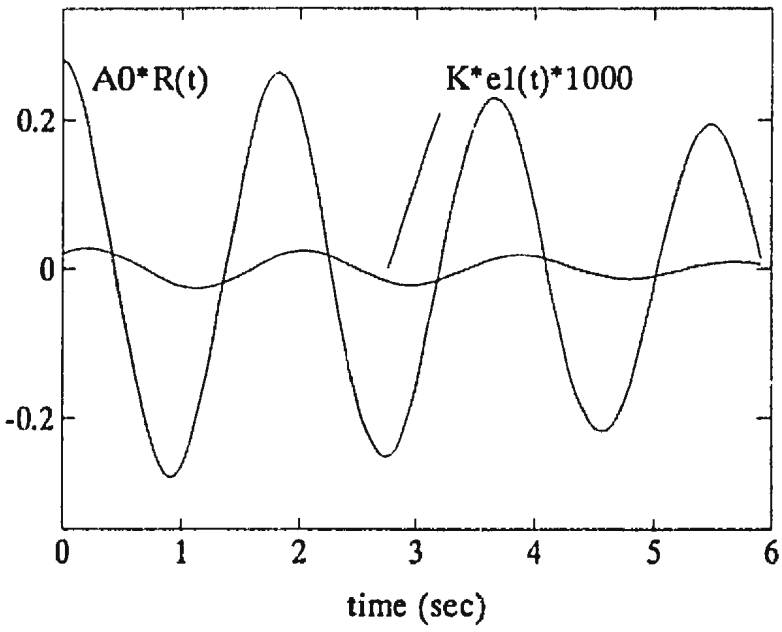

Figure 5.4: Comparison of magnitudes of crosscorrelation and autocorrelation

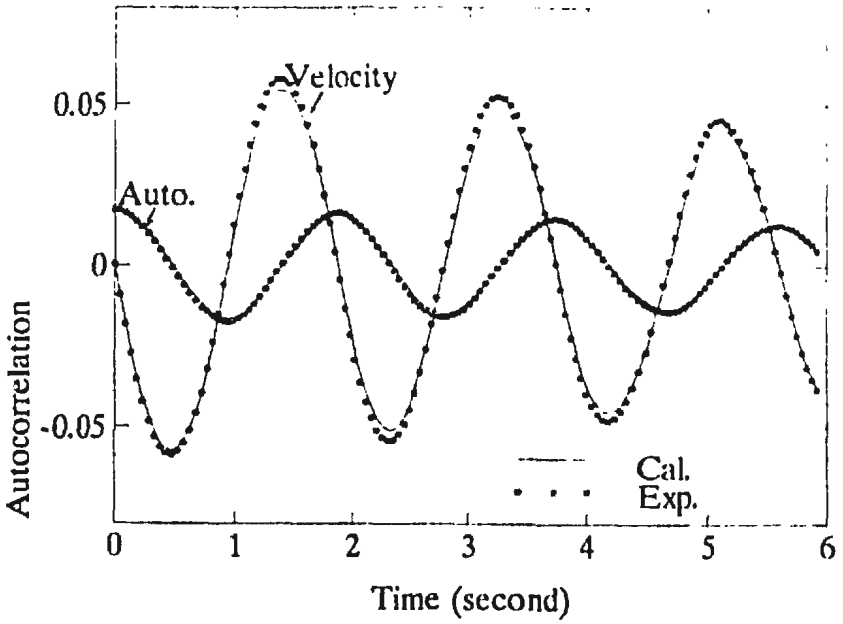

Figure 5.5: Comparison between calculated autocorrelation and experimental results for case A

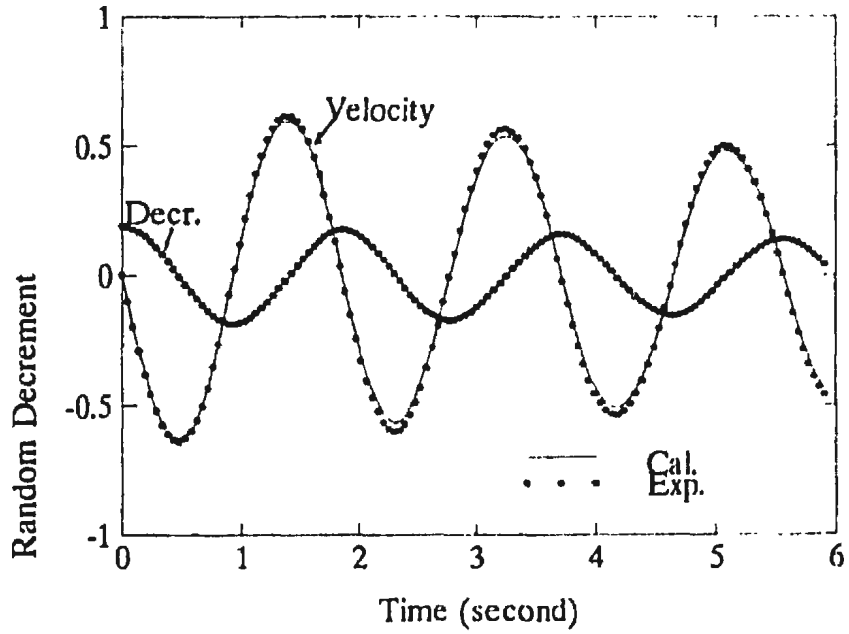

Figure 5.6: Comparison between calculated random decrement and experimental results for case C

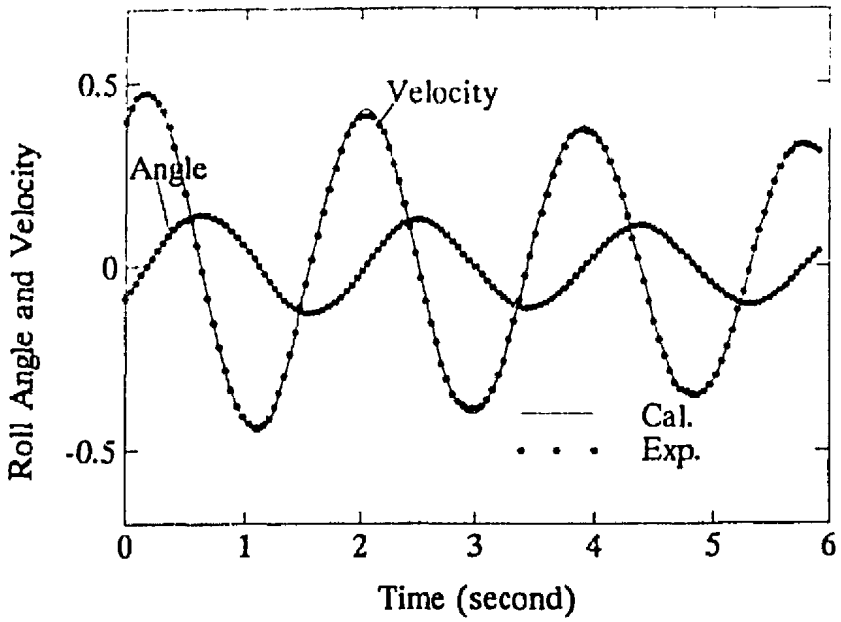

Figure 5.7: Comparison between calculated and experimental roll angle for case D

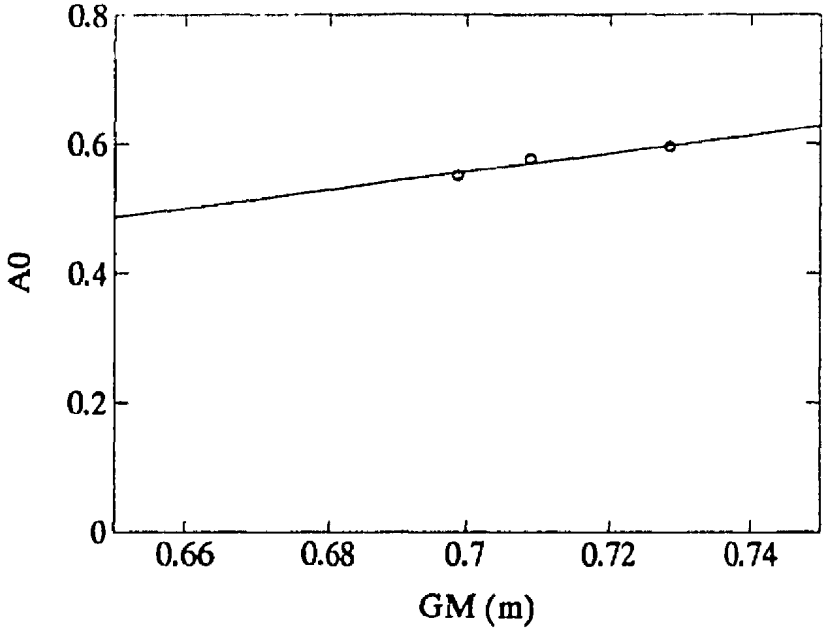

Figure 5.8: Relationship between GM and A_0 for full scale ship

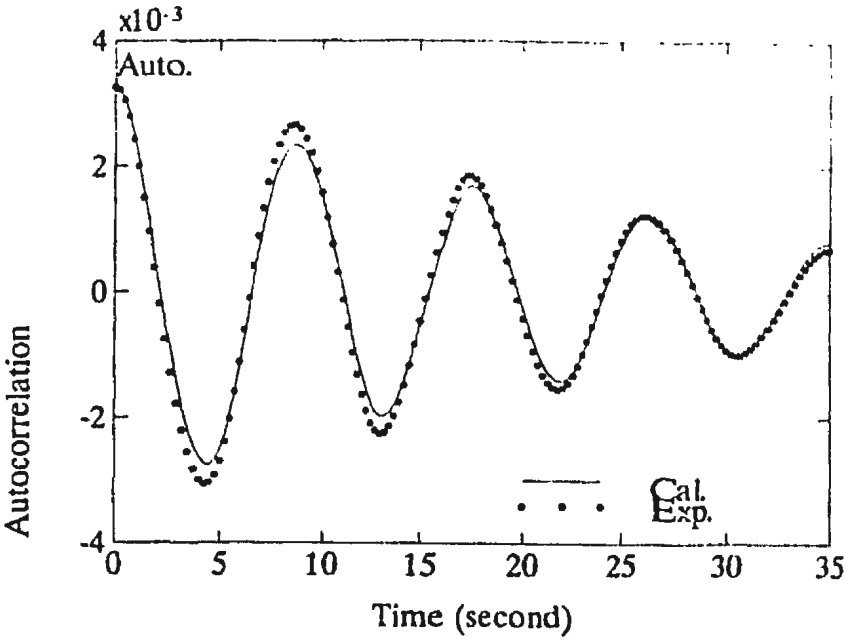

Figure 5.9: Comparison between calculated and experimental autocorelation of real ship (GM=0.6989)

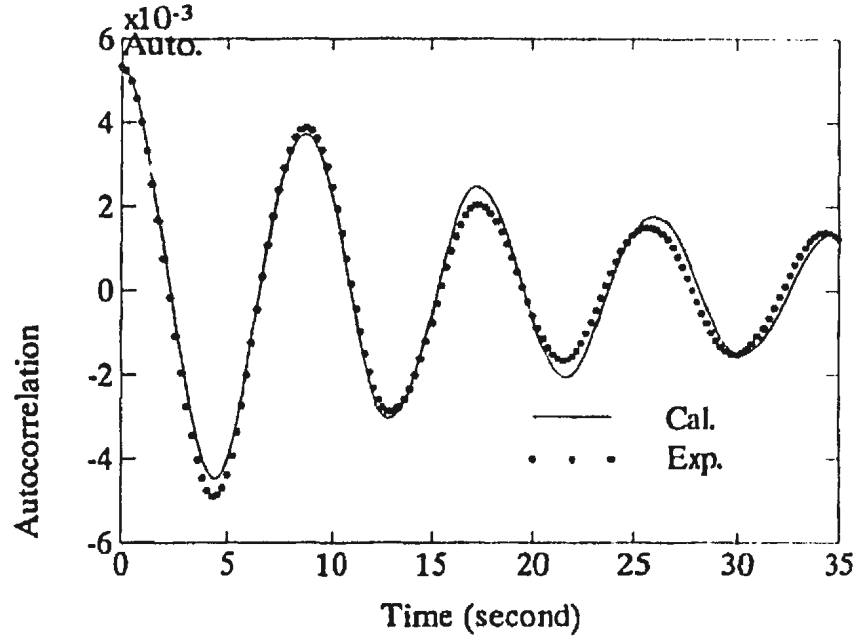

Figure 5.10: Comparison between calculated and experimental autocorelation of real ship (GM=0.7091)

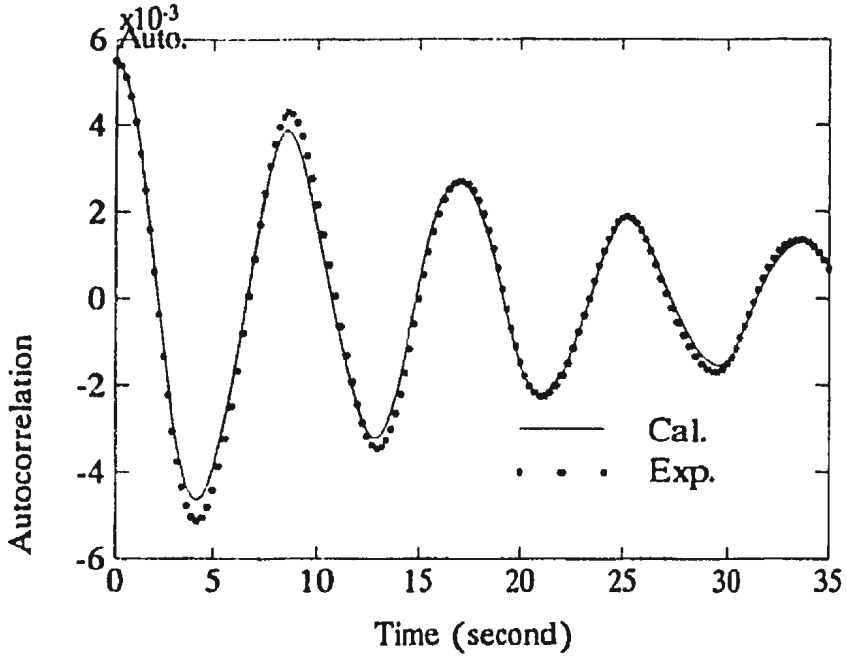

Figure 5.11: Comparison between calculated and experimental autocorelation of real ship (GM=0.7287)

Chapter 6

Probability distribution of Roll Motion

6.1 Introduction

In the previous Chapters, we have given a detailed report about how to estimate ship roll parameters. From these parameters, the ship roll stability can be assessed. For example, the restoring moment of the ship can be calculated from the parameters A_0, A_1, A_2. In this Chapter, we will discuss another way of assessing ship roll stability. From a statistical viewpoint, if the probability of the ship roll angle reaching a dangerous degree can be predicted, the ship roll stability can also be assessed. The objective of the present work is to find a method for the prediction of the joint probability distribution of roll angle and velocity. This can be used to obtain the probability distribution for roll angle, roll velocity and amplitude.

The ship roll motion can be modelled as a nonlinear random vibration problem. If the excitation can be idealized as a Gaussian white noise, a powerful tool: Markov vector approach can be used. In this case, the joint conditional probability density function of roll angle and velocity can be obtained from the solution of

a partial differential equation: the Fokker-Planck equation [17]. The analytical solution of this equation has been found only for very few simple cases. In this thesis, a numerical method was used to solve this equation. From the solution of the joint probability distribution of roll angle and roll velocity, the probability distribution of the amplitude of roll motion can be derived [18].

The method has been used for the analysis of the roll data from ship model tests and real ship measurements. The calculated probability distribution of roll angle, velocity and amplitude of roll motion are compared with the relevant histograms extracted from the measured data. The agreement between measured and estimated probability distribution is good. The numerical solution is also compared with the analytical solution for a special case of a *Duffing oscillator*. The agreement is excellent.

6.2 Markov Approximation and Solution

The governing equation of the roll motion of a ship in random waves can be written as:

$$\ddot{\varphi} + N(\dot{\varphi}) + Q(\varphi) = KM(t) \tag{6.1}$$

One can express the damping and restoration as:

$$N(\dot{\varphi}) = B_0\dot{\varphi} + B_1\dot{\varphi}|\dot{\varphi}| \tag{6.2}$$

$$Q(\varphi) = A_0\varphi + A_1\varphi^3 \tag{6.3}$$

Here $M(t)$ is assumed to be a Gaussian white noise with the mean and variance satisfying the following conditions [15]:

$$E(M(t)) = 0 \tag{6.4}$$

$$E(M(t_1)M(t_2)) = \delta(t_1 - t_2) \tag{6.5}$$

Let $\varphi = y_1$, $\dot{\varphi} = y_2$, equation (6.1) can be rewritten as:

$$\dot{Y} + G(Y) = F(t) \tag{6.6}$$

where

$$Y = \begin{Bmatrix} y_1 \\ y_2 \end{Bmatrix}$$

$$F = \begin{Bmatrix} 0 \\ KM(t) \end{Bmatrix}$$

$$G = \begin{Bmatrix} -y_2 \\ N(y_2) + Q(y_1) \end{Bmatrix}$$

If $F(t)$ is white noise, Y is a Markov vector and its joint conditional probability density function P satisfys Fokker-Planck equation:

$$\frac{\partial P}{\partial t} + \frac{\partial}{\partial y_1}(y_2 P) - \frac{\partial}{\partial y_2}[(N+Q)P] - \frac{K^2}{2}\frac{\partial^2 P}{\partial y_2^2} = 0 \tag{6.7}$$

where

$$P = P(y_1, y_2, t \mid y_{10}, y_{20}), \qquad y_{10} = y_1(0), \quad y_{20} = y_2(0)$$

and $P = P(y_1, y_2, t \mid y_{10}, y_{20})$ is the conditional probability density function with the condition that $y_1 = y_{10}, y_2 = y_{20}$ when time $t = 0$.

In the following, we will write P as a short form of $P = P(y_1, y_2, t)$.

No analytical solution is available for this equation when the damping is nonlinear, so we solve it by an approximate method — Galerkin method.

First, the variables are normalized using the following formulas:

$$\xi = \frac{y_1 - \mu_1(t)}{\sigma_1(t)} \qquad \eta = \frac{y_2 - \mu_2(t)}{\sigma_2(t)} \tag{6.8}$$

$\mu_1(t), \sigma_1(t), \mu_2(t), \sigma_2(t)$ are means and variances of $\varphi, \dot{\varphi}$ solved from the relevant linear roll equation of equation (6.1) while $A_1 = B_1 = 0$.

The weighted Hermite polynomials used in previous Chapters as modulating functions now are chosen as trial functions:

$$A^n(\xi) = e^{-\frac{\xi^2}{2}} H_n(\xi) = (-1)^n \frac{\partial^n}{\partial \xi^n}(e^{-\frac{\xi^2}{2}}) \qquad (n = 0, 1, 2, \ .....) \tag{6.9}$$

The advantage of such choice is due to th following recurrence and orthogonal properties of these functions:

$$\frac{\partial A^n}{\partial \xi} = -A^{n+1}(\xi) \tag{6.10}$$

$$\xi A^n(\xi) = A^{n+1}(\xi) + nA^{n-1}(\xi) \qquad (A^{-|n|} = 0) \tag{6.11}$$

and

$$\int_{-\infty}^{\infty} A^n(\xi) H_m(\xi) d\xi = n!\sqrt{2\pi}\delta_{m,n} \qquad (n \geq 0) \tag{6.12}$$

where $\delta_{m,n}$ is the Kronelker delta.

The next step is to expand the joint conditional probability density function P in terms of a set of trial functions.

$$P(y_1, y_2, t) = \sum_{k=0}^{m} \sum_{r=0}^{n} G^{kr}(t) A^k(\xi) A^r(\eta) \tag{6.13}$$

in which the coefficients $G^{kr}(t)$ are to be determined.

If equation (6.13) is the solution of the Fokker-Planck equation, it must satisfy the equation:

$$\int_{-\infty}^{\infty} \int_{-\infty}^{\infty} (\frac{\partial P}{\partial t} + \frac{\partial}{\partial y_1}(y_2 P)$$

$$-\frac{\partial}{\partial y_2}[(N+Q)P] - \frac{K^2}{2}\frac{\partial^2 P}{\partial y_2^2}) H_p(\xi) H_q(\eta) d\xi d\eta = 0 \tag{6.14}$$

This equation means that the residual of equation (6.7) is orthogonal to a set of linearly independent functions $H_p(\xi), H_q(\eta)$. As m, n approach to infinity, the residual vanishes and the Fokker-Planck equation is satisfied.

Integrating equation (6.14) and using the orthogonal condition (6.12), one can get a set of first-order differential equations:

$$\frac{\partial}{\partial t} G^{pq}(t) = \sum_{k=0}^{m} \sum_{r=0}^{n} f_{pqkr}(t) G^{kr}(t) \tag{6.15}$$
$$(p = 0, 1, 2, \ \ldots m, \quad q = 0, 1, 2, \ \ldots n)$$

$f_{pqkr}(t)$ are known functions and their expressions can be found in Appendix B. Equation (6.15) can be solved numerically under given initial conditions. If all coefficients $G^{kr}(t)$ are solved, the joint conditional probability density function of y_1, y_2 are known.

A common way of giving initial condition is to set,

$$P(y_1, y_2, 0) = \delta(y_1 - y_{10})\delta(y_2 - y_{20}) \tag{6.16}$$

In this case,

$$\begin{aligned}
&\int_{-\infty}^{\infty}\int_{-\infty}^{\infty} P(y_1, y_2, 0) H_p(\xi) H_q(\eta) d\xi d\eta \\
&= \int_{-\infty}^{\infty}\int_{-\infty}^{\infty} \delta(y_1 - y_{10})\delta(y_2 - y_{20}) H_p(\xi) H_q(\eta) \frac{d\xi}{dy_1}\frac{d\eta}{dy_2} dy_1 dy_2 \\
&= [H_p(\xi) H_q(\eta) \frac{d\xi}{dy_1}\frac{d\eta}{dy_2}]|_{t=0}
\end{aligned} \tag{6.17}$$

Using the orthogonal condition (6.12), another equation can be obtained:

$$\begin{aligned}
&\int_{-\infty}^{\infty}\int_{-\infty}^{\infty} P(y_1, y_2, t) H_p(\xi) H_q(\eta) d\xi d\eta \\
&= \sum_{k=0}^{m}\sum_{r=0}^{n}\int_{-\infty}^{\infty}\int_{-\infty}^{\infty} G^{kr}(t) A^k(\xi) A^r(\eta) H_p(\xi) H_q(\eta) d\xi d\eta \\
&= 2\pi p! q! G^{pq}(t)
\end{aligned} \tag{6.18}$$

Comparing equation (6.18) with equation (6.17), we get the initial condition as:

$$G^{pq}(0) = \frac{1}{2\pi p! q!}[H_p(\xi) H_q(\eta) \frac{d\xi}{dy_1}\frac{d\eta}{dy_2}]|_{t=0} \tag{6.19}$$

The ship roll problem can be considered as a stationary process. The joint probability density function of φ, $\dot{\varphi}$ can be found when time t approaches infinity:

$$lim_{t\to\infty} P(y_1, y_2, t \mid y_{10}, y_{20}) = p(y_1, y_2) = p(\varphi, \dot{\varphi}) \tag{6.20}$$

Other useful probability distribution and statistical measurements can be derived from the joint probability density function.

$$p(\varphi) = p(y_1) = \int_{-\infty}^{\infty} p(y_1, y_2) dy_2 = \sqrt{2\pi}\sigma_2 \sum_{k=0}^{m} G^{k0} A^k(\xi) \tag{6.21}$$

$$p(\dot{\varphi}) = p(y_2) = \int_{-\infty}^{\infty} p(y_1, y_2) dy_1 = \sqrt{2\pi}\sigma_1 \sum_{r=0}^{n} G^{0r} A^r(\eta) \tag{6.22}$$

and

$$E(\xi^2) = \int_{-\infty}^{\infty} p(\xi)\xi^2 dy_1 = 2\pi\sigma_1\sigma_2[G^{00} + 2G^{20}] \tag{6.23}$$

$$E(\eta^2) = \int_{-\infty}^{\infty} p(\eta)\eta^2 dy_2 = 2\pi\sigma_1\sigma_2[G^{00} + 2G^{02}] \tag{6.24}$$

6.3 Peak Statistics

As shown in Figure 6.1, letting $\nu_a^+ dt$ be the probability of such crossings as $\varphi(t)$ crossing a particular level $\varphi(t) = a$ from below to above in an interval of duration dt, we can see that if there is a crossing, it satisfies [21]

$$\frac{a - \varphi(t)}{dt} < \dot{\varphi}(t) < \infty \tag{6.25}$$

From Figure 6.2, it shows

$$\nu_a^+ dt = \int_0^{\infty} \int_{a-\dot{\varphi}dt}^{a} p(\varphi, \dot{\varphi}) d\varphi d\dot{\varphi} \tag{6.26}$$

Let $dt \to 0$, we find

$$\nu_a^+ = \int_0^{\infty} \dot{\varphi} p(a, \dot{\varphi}) d\dot{\varphi} \tag{6.27}$$

Further, for a narrow-band stationary random process such as ship roll response, the expected number of peaks per unit time above the level $\varphi(t) = a$ is equal to ν_a^+. The total expected number of peaks per unit time above the level $\varphi(t) = 0$ is ν_0^+. Hence from the relative frequency definition of probability, it follows that

$$P(\varphi(t) > a) = \frac{\nu_a^+}{\nu_0^+} \tag{6.28}$$

The probability density function for peaks is obtained by differentiation

$$p_a(a) = -\frac{dP}{da} = -\frac{1}{\nu_0^+}\frac{d\nu_a^+}{da} \tag{6.29}$$

Introducing the expressions (6.13), (6.27) into above equation, we have

$$p_a(a) = \frac{1}{\sigma_1}\frac{\sum_{k=0}^{m}\sum_{r=0}^{\frac{n}{2}} G^{k,2r} A^{k+1}(\xi_a)[H^{2r}(0) + 2rH^{2r-2}(0)]}{\sum_{k=0}^{m}\sum_{r=0}^{\frac{n}{2}} G^{k,2r} H^k(0)[H^{2r}(0) + 2rH^{2r-2}(0)]} \tag{6.30}$$

where

$$\xi_a = \frac{a - \mu_1}{\sigma_1}$$

6.4 Results and Discussion

6.4.1 Duffing's Equation

To illustrate the results of the previous sections, we first show the solution of a particular nonlinear system of the form of

Table 6.1: Parameters used in the calculation

Cases	m	n	B_0	A_0	A_1	K^2
A	8	8	1	10	5	2
B	8	8	1	10	20	2
C	12	12	1	10	20	2

$$\ddot{\varphi} + B_0\dot{\varphi} + A_0\varphi + A_1\varphi^3 = KM(t) \tag{6.31}$$

Equation (6.31) is called *Duffing's equation*. It has an analytical stationary solution for the joint probability density function, from which the analytical solution of the peak distribution can also be derived [22], [23].

Three test cases are carried out. The parameters used in each case are listed in Table 6.1.

In case A, the ratio of the nonlinear parameter A_1 to the linear parameter A_0 is 1/2. The 8th-order expansions of the joint probability distribution and the peak distribution give good approximations of the true solutions as indicated in Figure 6.3.

When the nonlinear parameter is twice the linear parameter in the case B, the 8th-order expansion of the joint probability distribution still gives a good approximation but the peak distribution approached to the same order is not so good (see Figure 6.4).

In the case C, when the order of the expansion is increased to 12 while roll parameters remain the same as that in the case B, the both approximations for joint probability distribution and peak distribution agree very well to the exact solutions as shown in Figure 6.5.

6.4.2 Measured Data

Second step to evaluate the present method is to apply it to the analysis of measured roll data from ship model tests and full scale ship measurements. The stationary solutions of the probability density functions $p(\varphi)$, $p(\dot{\varphi})$, $p_a(a)$ are calculated using $8th$-order expansion of trial functions. The histograms describing the same probability distribution are also calculated from the measured data.

For the experimental data of the ship model 366, the calculated probability distribution and the relevant histograms are shown in Figures 6.6 - 6.8. It shows that the present method gives very good approximation of the probability distribution of ship roll motion.

From the roll data measured on a full scale ship at sea, similar work is done. The good agreement is also observed between the predicted probability distribution and the histogram of measured date, as shown in Figures 6.9 - 6.11.

From these results, we can conclude that the present method is a good tool for the prediction of the probability distribution of ship roll motion.

The last problem is to explain why the white excitation assumption can be used without causing notable losses on the accuracy of the prediction. The reason is that the ship roll response is a narrow band process. For such a process, it only responses to the excitation with the frequency near ship's natural frequency, so the power spectrum of the excitation can be approximated by the constant value of the power spectrum at the ship's natural frequency.

From probability theory, if the excitation is nonwhite, but it can be generated as the response of a linear ordinary differential equation driven by white noise, the problem can also be solved by Markov approximation.

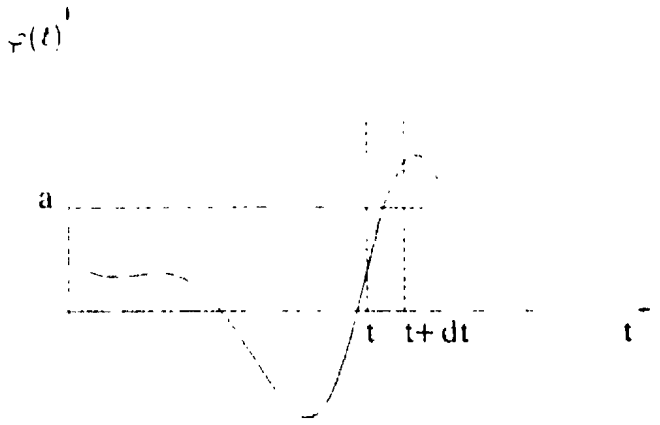

Figure 6.1: A-level crossing of $p(\varphi)$

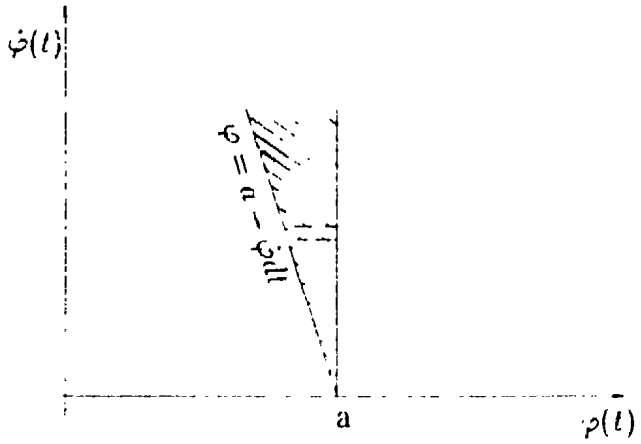

Figure 6.2: $\nu_a^+ dt = P(\frac{a-\varphi(t)}{dt} < \dot{\varphi}(t) < \infty)$

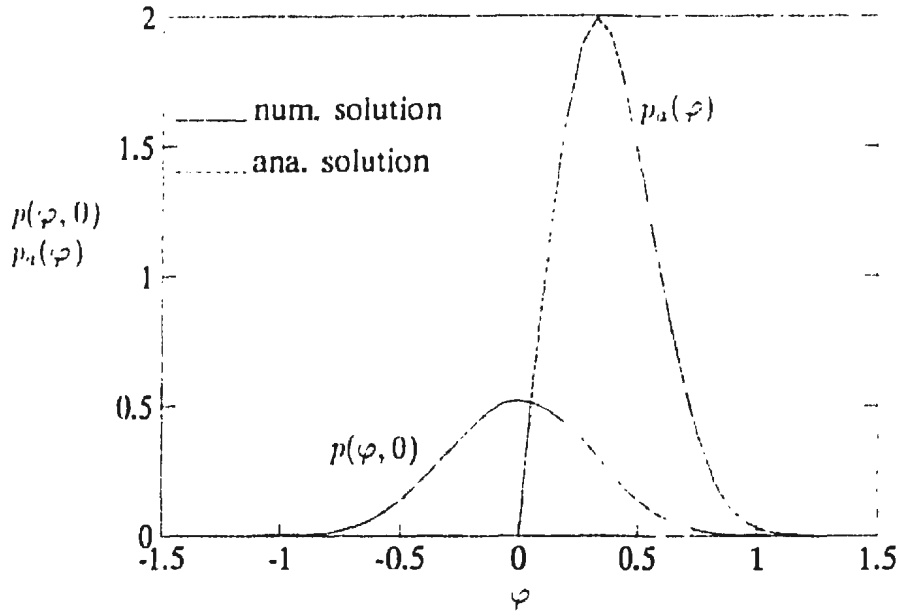

Figure 6.3: Comparison between estimated and analytical probability distribution for Case *A*

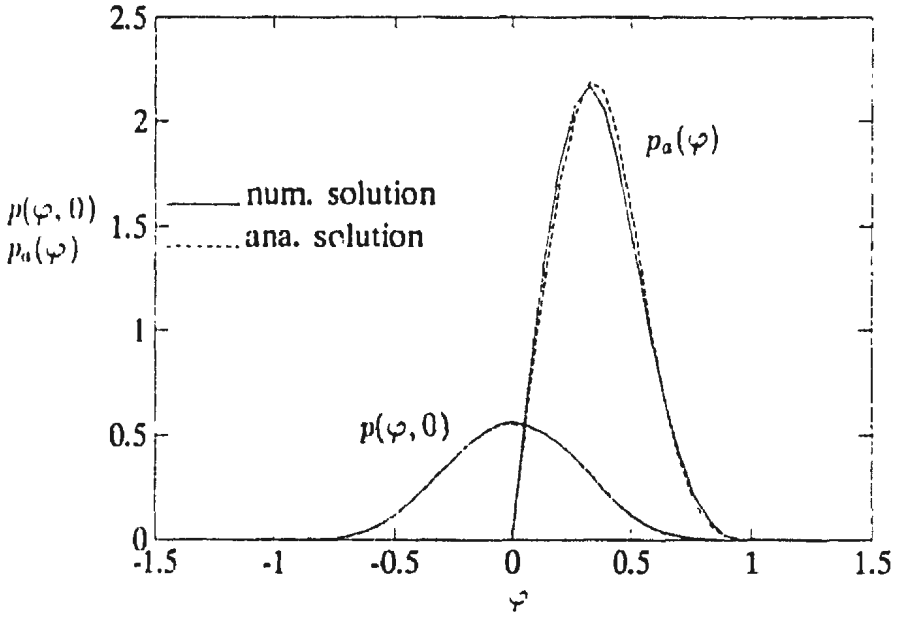

Figure 6.4: Comparison between estimated and analytical probability distribution for Case *B*

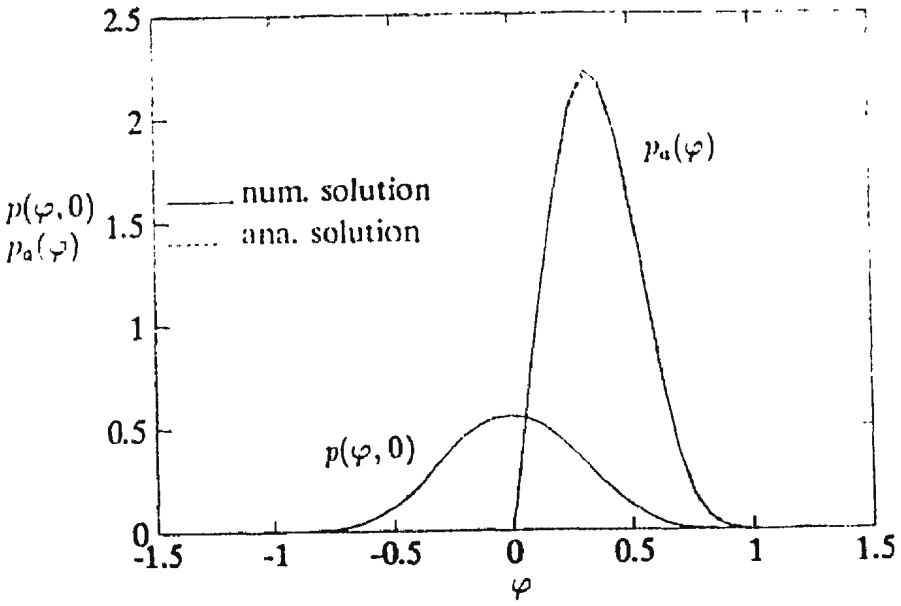

Figure 6.5: Comparison between estimated and analytical probability distribution for Case C

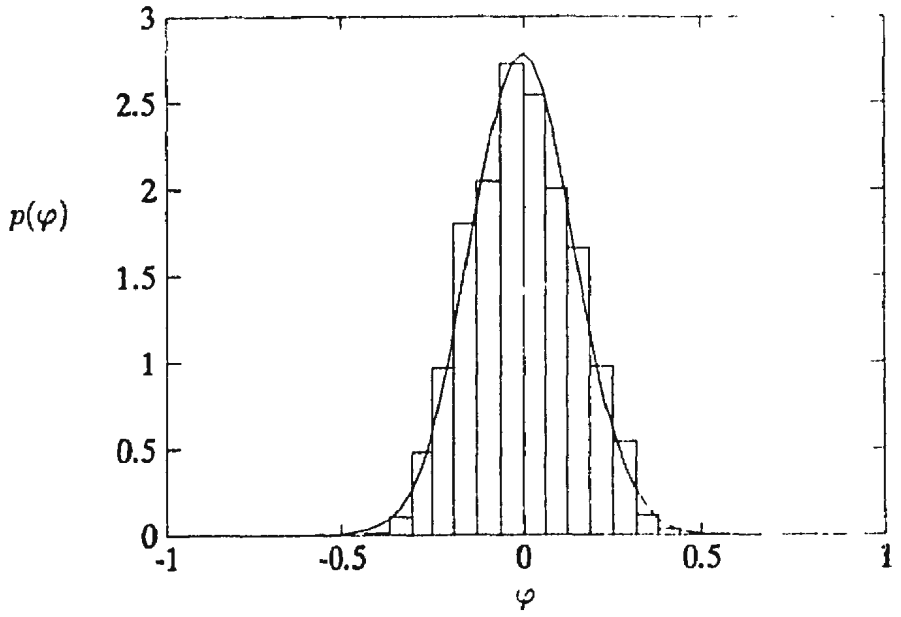

Figure 6.6: Comparison between estimated roll angle distribution to the histogram of measured data for Model 366

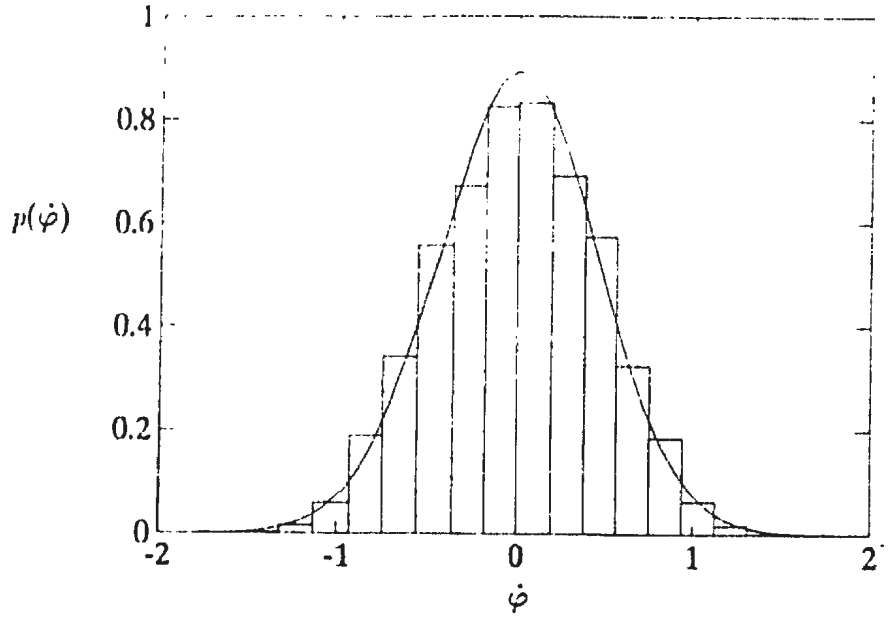

Figure 6.7: Comparison between estimated roll velocity distribution to the histogram of measured data for Model 366

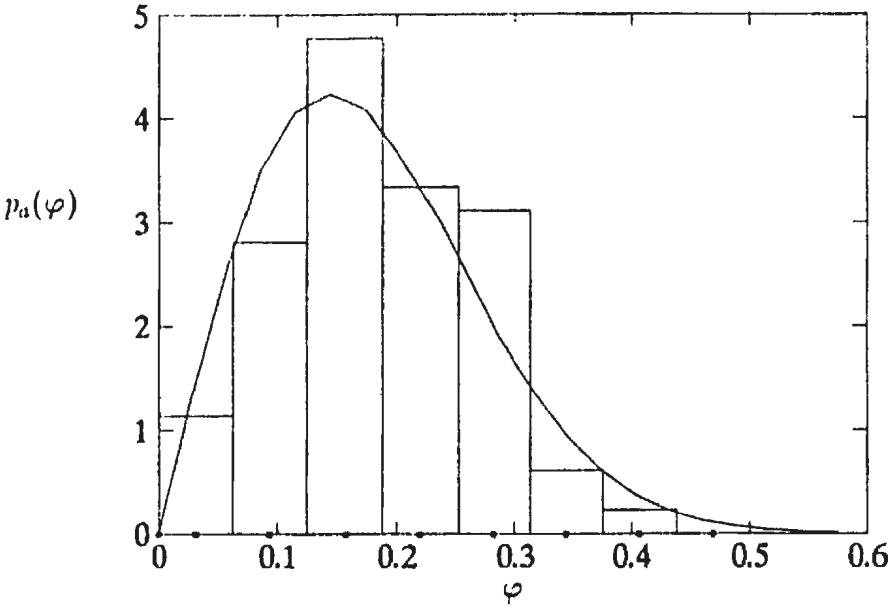

Figure 6.8: Comparison between estimated peak distribution to the histogram of measured data for Model 366

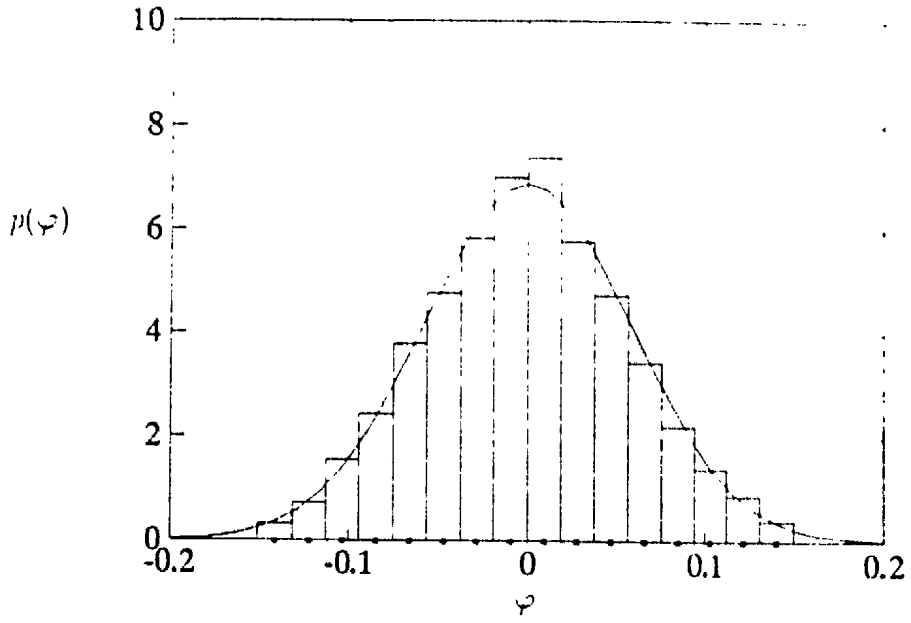

Figure 6.9: Comparison between estimated roll angle distribution to the histogram of measured data for full scale ship

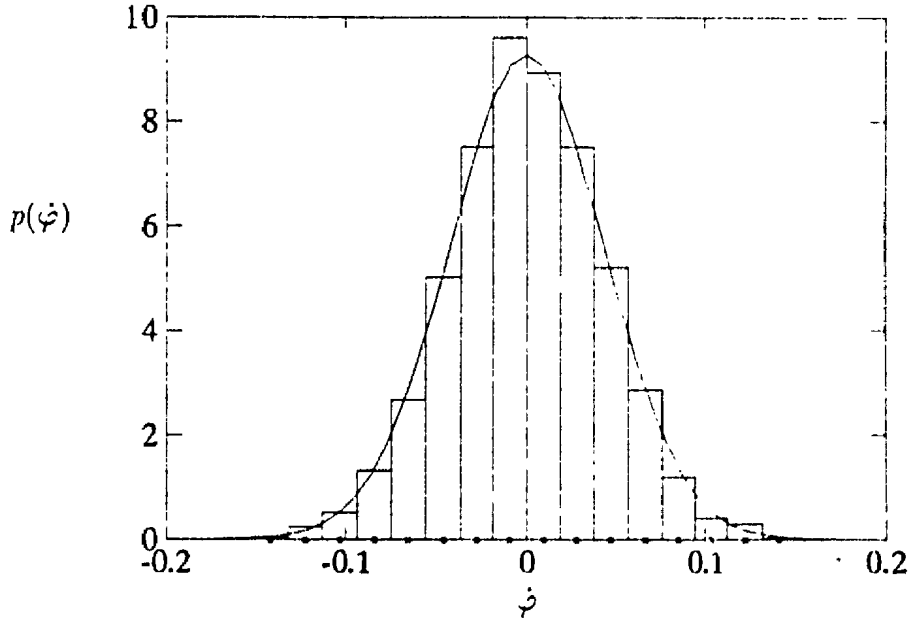

Figure 6.10: Comparison between estimated roll velocity distribution to the histogram of measured data for full scale ship

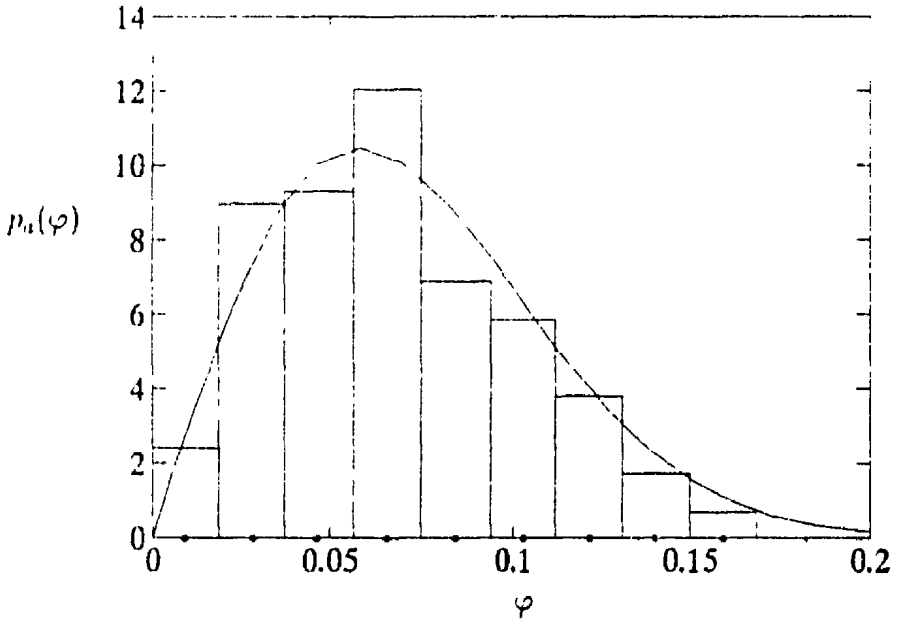

Figure 6.11: Comparison between estimated peak distribution to the histogram of measured data for full scale ship

Chapter 7

Conclusions

A new method for the parametric identification of ship roll motion is proposed. From the estimated roll parameters, the probability distributions of roll angle, roll velocity and the peaks of the roll motion are derived and calculated by numerical approximation. Thus, a systematic study of ship roll motion based on the measured roll data is given.

From the theoretical basis of the proposed method and the results it has produced so far, this new method shows some advantages over other existing parametric identification methods for ship roll problems. These advantages are:

1. The accuracy of the estimation of this method is higher than some current methods because it avoids one of the main sources of error, that is numerical differentiation of the measured data. The numerical integration instead of the numerical differentiation is used in the new method to formulate the equations for the parametric solution. As it is well known, the numerical integration can smooth the noise in the measured data while the numerical differentiation enlarges it.

2. The proposed method does not need such assumptions used in some meth-

ods as light damping, white noise excitation, and equivalent linearization, and therefore it does not place many restrictions on the form of roll equation. As long as the parameters can be separated from the function of time, all the parameters can be estimated with higher accuracy. The parameters of nonlinear damping, nonlinear-time-dependent restoring moment and the strength of excitation can be estimated at the same time without iterations.

3. The method does not need very long record for the parametric identification.

In addition to above mentioned advantages, the method can be applied to the prediction of roll parameters of a full scale ship at sea without knowing the wave measurements, because all estimation is obtained from measured roll response only.

A numerical approach was used to solve the probability distributions of ship roll motion from the estimated parameters. The calculated results of the probability distributions of roll angle, roll velocity and peaks of roll motion indicated such an approach was also satisfactory.

References

[1] Froude, W., "The Papers of William Froude," The Royal Institution of Naval Architects, 1955

[2] Roberts, J. B., "Estimation of Nonlinear Ship Roll Damping from Free-Decay Data," Journal of Ship Research, Vol. 29 No. 2, pp. 127-138, 1985

[3] Spouge, J. R., "Non-linear Analysis of Large Amplitude Roll Experiments," International Shipbuilding Progress, Vol. 35, No 403, pp. 271-324, 1988

[4] Bass, D. W. and Haddara, M. R., "Nonlinear Models of Ship Roll Damping," International Shipbuilding Progress, Vol. 35, No 401, pp. 5-24, 1988

[5] Bass, D. W. and Haddara, M. R., "Roll and Sway-Roll Damping for Three Small Fishing Vessels," International Shipbuilding Progress, Vol. 38, No 413, pp. 51-57, 1991

[6] Gawthrop, P. J., Kountzeris, A., and Roberts, J. B., " Parametric Identification of Nonlinear Ship Roll Motion from Forced data," Journal of Ship Research, Vol., 132, No. 2, pp. 101-111, 1988

[7] Haddara, M. R., "Parametric Identification of Rolling Motion," Workshop on the Stability of Low L/B Hull Forms, Institute of Marine Dynamics, LM-HYD-78, St. John's, Canada, 1988

[8] Zhang, Y. and Haddara, M. R., "Parametric Identification of Nonlinear Roll Motion from Roll Response", Accepted by International Shipbuilding Progress.

[9] Kountzeris, A., Roberts, J. B. and Gawthrop, P. J., "Estimation of Ship Roll Parameters from Motion in Irregular Seas," Transactions of the Royal Institution of Naval Architects, Vol. 132, pp. 253-266, 1991

[10] Roberts, J. B., Dunne, J. F. and Debonos, A., "Estimation of Ship Roll Parameters in Random Waves," Proceedings, 10th International Conference on Offshore Mechanics and Arctic Engineering, Vol. II, Safety and Reliability, pp. 97-106, 1991

[11] Haddara, M. R., "On the Random Decrement for Nonlinear Rolling Motion," Proceedings, 11th International Conference on Offshore Mechanics and Arctic Engineering, Vol II, Safety and Reliability, pp. 321-324, 1992

[12] Wu X., "Roll Motion Parameter Identification Using Response in Random Waves" Masters Thesis, Memorial University of Newfoundland, 1993

[13] Haddara, M. R. and Zhang, Y., "Roll Damping Identification for Ships at Sea," To be published

[14] Loeb, J. M. and Cahen, G. M., "More about Process Identification," IEEE Trans., AC-10, pp. 359-361, 1965

[15] Caughey, T. K., "Derivation and Application of the Fokker-Planck Equation to Discrete Nonlinear Dynamic System Subjected to White Random Excitation", Journal of the Acoustical Society of America, Vol. 35, No. 11, pp. 1683-1692, 1963

[16] Caughey, T. K., "On the Response of a Class of Nonlinear Oscillators to Stochastic Excitition", Proceedings, Colloquium International du Centre National de la Recherche Scientifique, No. 148, Marseille, France, Sep., 1964

[17] Haddara, M. R., "A Modified Approach for the Application of Fokker-Planck Equation to the Nonlinear Ship Motions in Random Waves," International Shipbuilding Progress, Vol. 21, No. 242, pp. 283-288, 1974

[18] Haddara, M. R. and Zhang Y., "On the Joint Probability Density Function of Nonlinear Rolling Motion ", Accepted by Journal of Sound and Vibration

[19] Haddara M. R. and P. Bennett, " On the Damping Identification for Nonlinear Oscillatory System", International Shipbuilding Progress, Vol. 13, No. 1/2, pp. 45-51, 1989

[20] Ibrahim, S. R., "Random Decrement Technique for Model Identification of Structures", AIAA Journal of Spacecraft and Rockets, Vol. 14, No. 11, pp. 696 - 700, 1977

[21] Crandall, S. H., "Zero Crossings, Peaks, and Other Statistical Measures of Random Responses", Journal of the Acoustical Society of America, Vol. 35, No. 11, pp. 1693-1699, 1963

[22] Crandall, S. H., "The Envelope of Random Vibration of a Lightly Damped Nonlinear Oscillator," Proceedings, 2nd Conference of Nonlinear Vibrations, Warsaw, Sep. 1962

[23] Lyon, R. H., "On the Vibration Statistics of a Randomly Excited Hard Spring Oscillator," Journal of the Acoustical Society of America, Vol. 32, pp. 716-719, 1960

Appendices

Appendix A

A and B Matrixes

$$B = -[\overline{\Psi_2(\varphi)}, \overline{\Psi_3(\varphi)}, \overline{\Psi_4(\varphi)}, \overline{\Psi_5(\varphi)}, \overline{\Psi_6(\varphi)}, \overline{\Psi_7(\varphi)}, \overline{\Psi_8(\varphi)}, \overline{\Psi_9(\varphi)}, \overline{\Psi_{10}(\varphi)}, \ldots, \overline{\Psi_{9+m}(\varphi)}, \overline{\Psi_{9+m+1}(\varphi)}, \ldots, \overline{\Psi_{9+2m}(\varphi)}]^T$$

$$
\mathbf{A} = \begin{bmatrix}
\overline{\overline{(\varphi)}}_1 & (\dot{\varphi}|\dot{\varphi}|)_0 & (\varphi)_0 & (\varphi^3)_0 & (\varphi^5)_0 & (sin(\omega t)\varphi)_0 & (sin(\omega t)\varphi^3)_0 \\
\cdots & \cdots & \cdots & \cdots & \cdots & \cdots & \cdots \\
\overline{\overline{(\varphi)}}_9 & (\dot{\varphi}|\dot{\varphi}|)_8 & (\varphi)_8 & (\varphi^3)_8 & (\varphi^5)_8 & (sin(\omega t)\varphi)_8 & (sin(\omega t)\varphi^3)_8 \\
\cdots & \cdots & \cdots & \cdots & \cdots & \cdots & \cdots \\
\overline{\overline{(\varphi)}}_{8+m} & (\dot{\varphi}|\dot{\varphi}|)_{7+m} & (\varphi)_{7+m} & (\varphi^3)_{7+m} & (\varphi^5)_{7+m} & (sin(\omega t)\varphi)_{7+m} & (sin(\omega t)\varphi^3)_{7+m} \\
\overline{\overline{(\varphi)}}_{9+m} & (\dot{\varphi}|\dot{\varphi}|)_{8+m} & (\varphi)_{8+m} & (\varphi^3)_{8+m} & (\varphi^5)_{8+m} & (sin(\omega t)\varphi)_{8+m} & (sin(\omega t)\varphi^3)_{8+m} \\
\cdots & \cdots & \cdots & \cdots & \cdots & \cdots & \cdots \\
\overline{\overline{(\varphi)}}_{8+2m} & (\dot{\varphi}|\dot{\varphi}|)_{7+2m} & (\varphi)_{7+2m} & (\varphi^3)_{7+2m} & (\varphi^5)_{7+2m} & (sin(\omega t)\varphi)_{7+2m} & (sin(\omega t)\varphi^3)_{7+2m}
\end{bmatrix}
$$

$$
\begin{bmatrix}
(sin(\omega t)\varphi^5)_0 & (sin(\Omega_1 t))_0 & \cdots & (sin(\Omega_m t))_0 & (cos(\Omega_1 t))_0 & \cdots & (cos(\Omega_m t))_0 \\
\cdots & \cdots & \cdots & \cdots & \cdots & \cdots & \cdots \\
(sin(\omega t)\varphi^5)_8 & (sin(\Omega_1 t))_8 & \cdots & (sin(\Omega_m t))_8 & (cos(\Omega_1 t))_8 & \cdots & (cos(\Omega_m t))_8 \\
\cdots & \cdots & \cdots & \cdots & \cdots & \cdots & \cdots \\
(sin(\omega t)\varphi^5)_{7+m} & (sin(\Omega_1 t))_{7+m} & \cdots & (sin(\Omega_m t))_{7+m} & (cos(\Omega_1 t))_{7+m} & \cdots & (cos(\Omega_m t))_{7+m} \\
(sin(\omega t)\varphi^5)_{8+m} & (sin(\Omega_1 t))_{8+m} & \cdots & (sin(\Omega_m t))_{8+m} & (cos(\Omega_1 t))_{8+m} & \cdots & (cos(\Omega_m t))_{8+m} \\
\cdots & \cdots & \cdots & \cdots & \cdots & \cdots & \cdots \\
(sin(\omega t)\varphi^5)_{7+2m} & (sin(\Omega_1 t))_{7+2m} & \cdots & (sin(\Omega_m t))_{7+2m} & (cos(\Omega_1 t))_{7+2m} & \cdots & (cos(\Omega_m t))_{7+2m}
\end{bmatrix}
$$

Note: $\Psi_n(\ )$ has been written as $(\ )_n$ in matrix A.

Appendix B

Expression for $\frac{\partial}{\partial t}(G^{p,q})$

$$\frac{\partial}{\partial t}(G^{p,q}) =$$
$$-c_0 G^{p-1,q} - c_1 G^{p-2,q} - c_1(p+1)G^{p,q}$$
$$-d_0 G^{p,q-1} - d_1 G^{p,q-2} - d_1(q+1)G^{p,q}$$
$$-\frac{\mu_2}{\sigma_1} G^{p-1,q} - \frac{\sigma_2}{\sigma_1}[G^{p-1,q-1} + (q+1)G^{p-1,q+1}]$$
$$-v_0 G^{p,q} - v_1[G^{p,q-1} + (q+1)G^{p,q+1}]$$
$$-v_2[G^{p,q-2} + (2q+1)G^{p,q} + (q+2)(q+1)G^{p,q+2}] + \frac{c_0 + s_0}{\sigma_2} G^{p,q-1}$$
$$+\frac{c_1}{\sigma_2}[G^{p-1,q-1} + (p+1)G^{p+1,q-1}] + \frac{s_1}{\sigma_2}[G^{p,q-2} + (q+1)G^{p,q}]$$
$$+\frac{c_2}{\sigma_2}[G^{p-2,q-1} + (2p+1)G^{p,q-1} + (p+2)(p+1)G^{p+2,q-1}]$$
$$+\frac{c_3}{\sigma_2}[G^{p-3,q-1} + 3pG^{p-1,q-1} + 3(p+1)^2 G^{p+1,q-1} + (p+3)(p+2)(p+1)G^{p+3,q-1}]$$
$$+\frac{s_2}{\sigma_2}[G^{p,q-3} + (2q+1)G^{p,q-1} + (q+2)(q+1)G^{p,q+1}]$$
$$+\frac{s_3}{\sigma_2}[G^{p,q-4} + 3qG^{p,q-2} + 3(q+1)^2 G^{p,q} + (q+3)(q+2)(q+1)G^{p,q+2}]$$
$$-\frac{\Psi_0}{2{\sigma_2}^2} G^{p,q-2}$$

$$(G^{p,q} = 0, \quad if \ \ p < 0 \ \ or \ \ q < 0 \ \ or \ \ p > m \ \ or \ \ q > n)$$

Appendix C

Data of Ship Models and Full Scale Ship

Table C.1: Particulars of ship models

Models	363	365	366	367
Scale	1:12	1:9.1	1:6.8	1:13
LWL(m)	1.551	1.336	1.568	1.389
Beam(m)	0.507	0.542	0.506	0.492
Draft(m)	0.221	0.215	0.205	0.188
LCB(m)	-1.09	-0.052	-0.138	-0.052
Mass(kg)	80	55	69.5	64.4
GM(m) at OG=0	0.031	0.033	0.045	0.038
ω (r/s) at OG=0	2.74	3.27	3.18	3.45
α_1 at OG=0	1.2832	-0.3851	0.2024	1.6068
α_2 at OG=0	-1.3293	-2.5141	-1.8402	-2.2615

Table C.2: General particulars of a full scale ship

Vessel Name	Newfoundland Alert
Type of Vessel	Fishing Vessel
Length Between Perpendicular	32.80 (m)
Breadth Moulded	10.00 (m)
Depth Moulded	6.80 (m)
Summer Load Draft	4.01 (m)
Displacement at S.L.W.L.	673 (ton)
Lightship Weight	406 (ton)
Date Keel Laid	February 25, 1988
Builder	Marystown Shipyard Limited

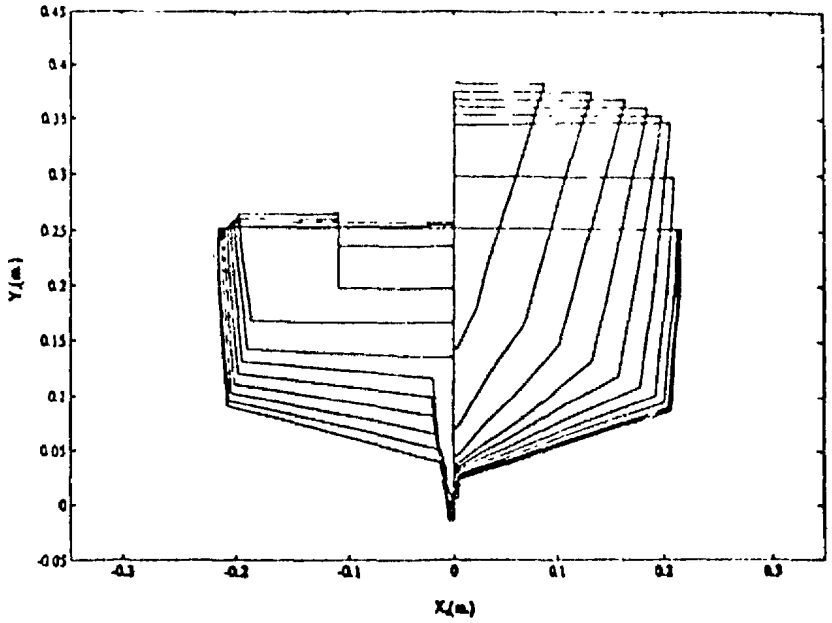

Figure C.1: Body plan of Model 363

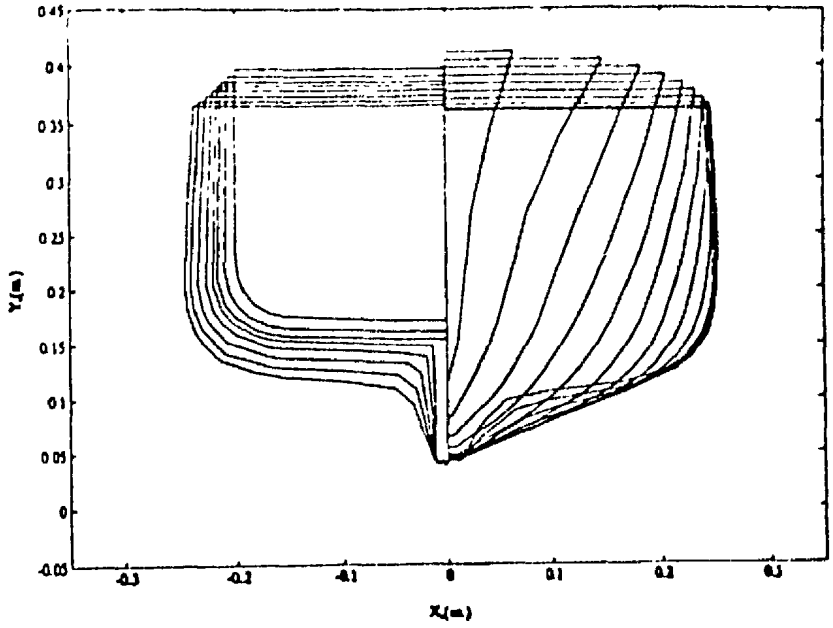

Figure C.2: Body plan of Model 365

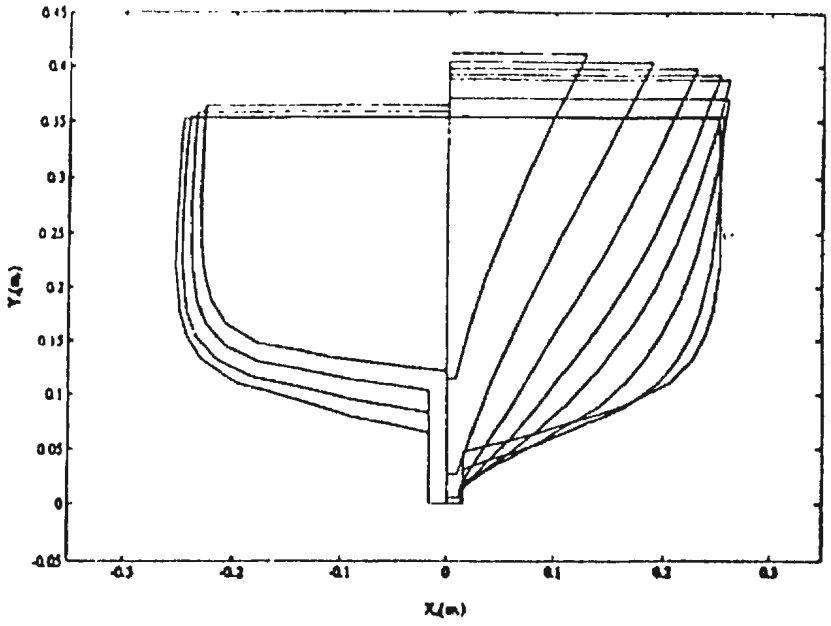

Figure C.3: Body plan of Model 366

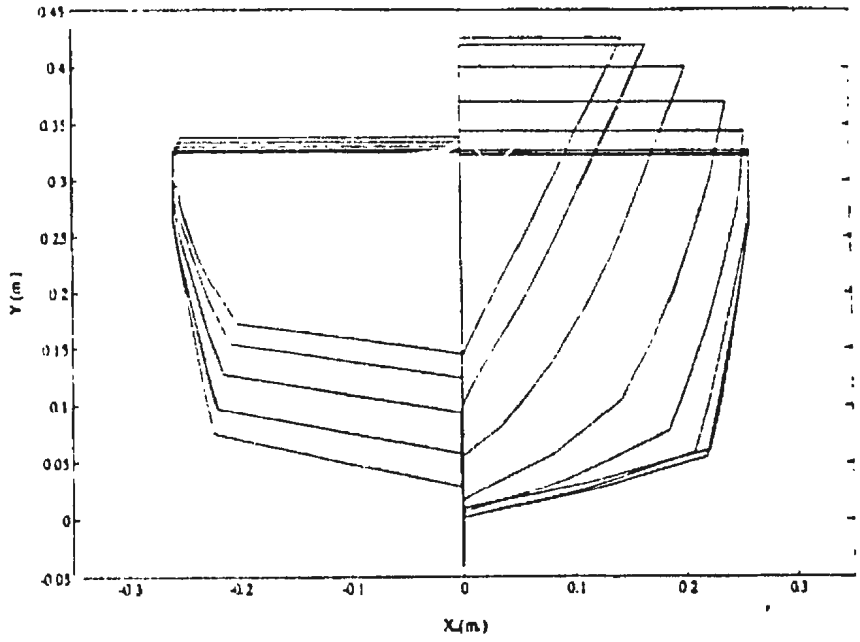

Figure C.4: Body plan of Model 367

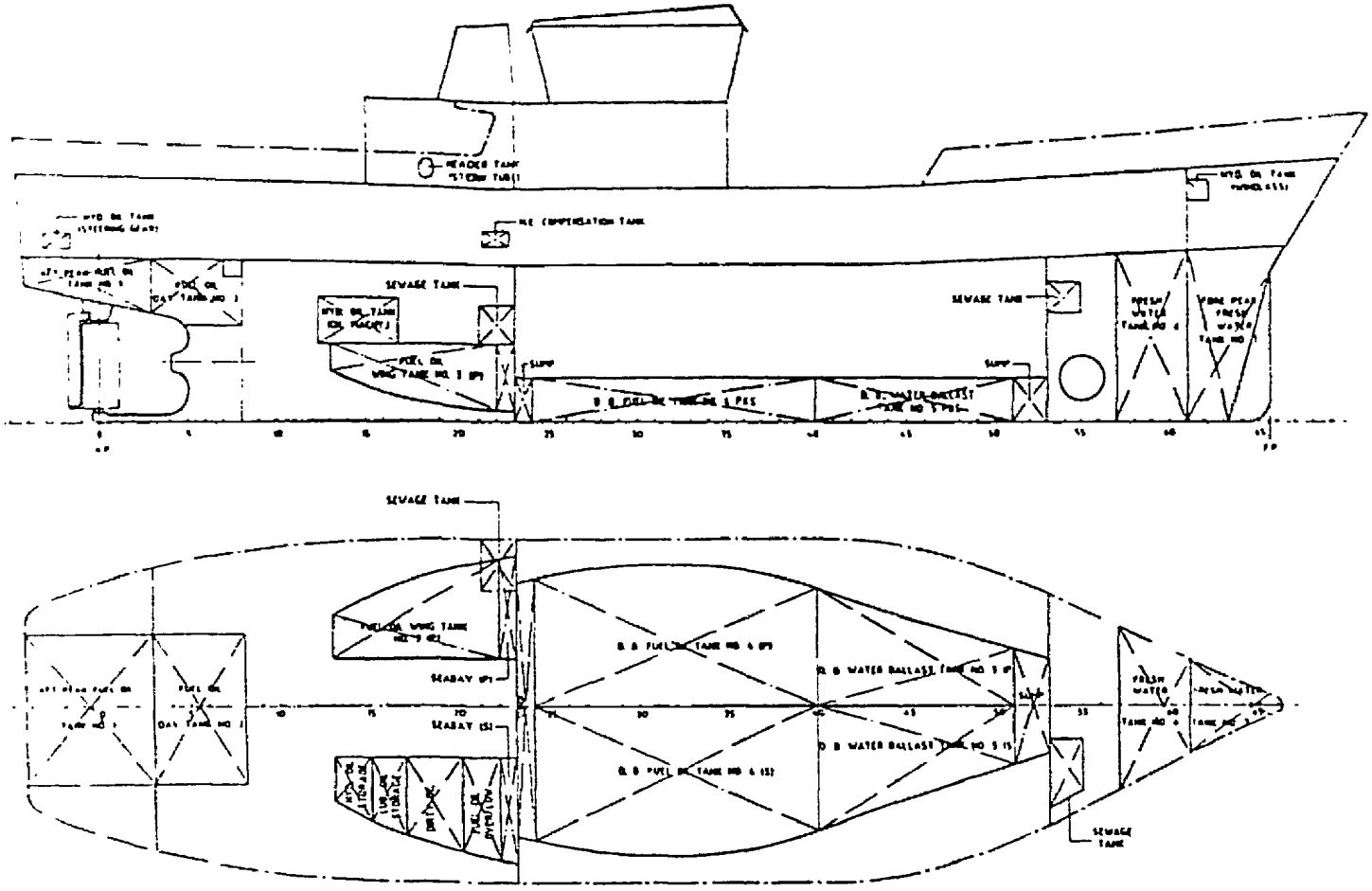

Figure C.5: Full scale ship layout